	Note on Virgo Parabolic telescope	Date 09/2010 VIR-0504A-10 Page 1 of 59
---	-----------------------------------	--



**Note on Virgo Parabolic telescope: Design, installation and
commissioning**

Authors:

P.La Penna, O. Francois, J. Marque, E. Genin

Date :

15/09/2010

CHANGE RECORD


<i>Issue/Rev</i>	<i>Date</i>	<i>Section affected</i>	<i>Reason/ remarks</i>

Authors	Institute	Signature
P. La Penna	EGO	
O. Francois	EGO	
J. Marque	EGO	
E. Genin	EGO	
Approved by :		



Summary:

1. INTRODUCTION.....	6
2. OVERVIEW OF VIRGO SUSPENDED INJECTION BENCH (SIB).....	7
2.1. GUIDELINES FOR THE DESIGN	7
2.2. OPTICAL DESIGN	7
2.3. MECHANICAL DESIGN.....	9
3. TELESCOPE TRADE-OFF ANALYSIS	12
3.1. REFRACTIVE TELESCOPE (E.G. T1)	12
3.1.1. <i>T1 design</i>	12
3.1.2. <i>Off the shelf/off the shelf lens based telescope: our choice for the next IB</i>	13
3.1.2.1 Performances: imaging	14
3.1.2.2 Performances: gaussian optics	15
3.2. DESIGN OF THE T2 TELESCOPE	17
3.2.1. <i>Spherical mirrors telescope with refractive telescope T1</i>	17
3.2.1.1 Proposed optical design	17
3.2.1.2 Gaussian optics	19
3.2.2. <i>Parabolic off-axis mirrors telescope (simulation with T1)</i>	23
3.2.2.1 Proposed optical design	23
3.2.2.2 Gaussian optics	25
3.2.2.3 Influence of M6 (surf. 16) clear aperture on the beam profile @ 3km.....	29
4. THERMAL LENSING	31
4.1. THERMAL LENSING COMPENSATION BY ADJUSTING T1 SEPARATION	34
4.2. THERMAL LENSING COMPENSATION BY ADJUSTING T2 SEPARATION	37
5. COMPENSATION OF MC CURVATURE ERRORS	39
5.1. COMPENSATION WITH T1 SEPARATION.....	39
5.2. COMPENSATION WITH T2 SEPARATION.....	40
5.3. COMPENSATION WITH T1 AND T2 SEPARATIONS	40
5.4. COMPENSATING BY REPLACING THE T1 FIRST LENS	41
6. PARABOLIC TELESCOPE (T2) PRE-ALIGNMENT.....	42
6.1. SINGLE PASS METHOD WITH TWO AUTOCOLLIMATORS	42
6.2. FIGURE 34: STEP 3: THE SINGLE PASS METHOD DOUBLE PASS METHOD WITH A SINGLE AUTOCOLLIMATOR AND A COUPLE LASER/BEAM EXPANDER.	45
7. COMMISSIONING OF THE PARABOLIC TELESCOPE.....	49
7.1. OVERVIEW OF THE COMMISSIONING	49
7.2. USE OF ZEMAX SOFTWARE DURING THE TELESCOPE OPTIMIZATION PROCESS: EXAMPLE 1.	50
7.3. USE OF ZEMAX SOFTWARE FOR MATCHING ADJUSTMENT ON VIRGO+: EXAMPLE 2.	52
8. APPENDIX A: PARABOLIC MIRRORS OPTICAL CHARACTERIZATION	54

	<p>Note on Virgo Parabolic telescope</p>	<p>Date 09/2010 VIR-0504A-10 Page 4 of 59</p>
---	--	---

8.1. M5 MIRROR 54

8.2. M6 MIRROR 55

9. APPENDIX B : MIRRORS MECHANICAL MOUNTS..... 56

10. APPENDIX C : ACTUATORS..... 57

9.1. PLANE MIRROR ACTUATORS 57

9.2. PARABOLIC MIRROR ANGULAR ACTUATORS 57

9.3. LENS TRANSLATOR..... 58


9.4. PZT FOR THE RFC STEERING MIRRORS 58

11. REFERENCES..... 59



List of abbreviations


IB	Injection bench
FI	Faraday isolator
MF	Merit function: feature in Zemax to optimize parameters.
MTF	Modulation Transfer Function
IMC	Input Mode cleaner
RFC	Reference Cavity
T1	Reducing telescope: used to adapt the MC waist size to the FI clear aperture
T2	Interferometer mode matching telescope.
INJ tower	Injection tower

	Note on Virgo Parabolic telescope	Date 09/2010 VIR-0504A-10 Page 6 of 59
---	-----------------------------------	--

1. Introduction

The input mode matching telescope (MMT) of Virgo is required to enlarge the beam by a factor of 8 (beam waist = 2.6 mm, beam waist in the interferometer = 21 mm). There are only two possibilities to do this without introducing large spherical aberrations: either a 2-m-long folded refractive telescope, analogous to those mounted on the Detection Bench, or a compact refractive off-axis parabolic telescope. The refractive lens telescope would produce reflections from its AR coated surfaces, which could affect the interferometer sensitivity by adding phase noise due to spurious beams. The lenses cannot be misaligned by a significant amount, without introducing large astigmatism of the beam. Moreover, space constraints on the suspended injection bench (SIB) are critical. For these reasons it was decided to use a reflective off-axis parabolic telescope: the design showed that, when properly aligned, this telescope would have been almost aberration free. At the moment of the Injection Bench design the level of aberration was fixed in order not to have a mismatching with the interferometer bigger than 4 % (at least 96% matching). The installed off-axis parabolic telescope has matched this requirement. When properly aligned and centered the mismatching can be less than 1.5%.

First of all, we will give an overview of Virgo Suspended Injection Bench installed in Fall 2005. The second part of the document will be devoted to a description of the design process of the SIB telescopes and the expected performances. Then the use of these telescopes to compensate for thermal effects and Mode-cleaner end mirror radius of curvature error will be evaluated in order to define the kind and the range of the actuators that should be installed on T1 and T2 telescopes optics. Methods used to pre-align the parabolic telescope will be given. Finally, a few examples of commissioning of the parabolic telescope will be presented.

	Note on Virgo Parabolic telescope	Date 09/2010 VIR-0504A-10 Page 7 of 59
---	-----------------------------------	--

2. Overview of Virgo Suspended Injection Bench (SIB)

2.1. Guidelines for the design

At the time the new Suspended Injection Bench (SIB) has been designed (2004-2005) the main issue to solve was to be able to run the injection system and the Interferometer at full power (10 W at that time). In order to suppress fringes visible in the IMC cavity that were disturbing the MC and interferometer control, a Faraday isolator had to be installed between the IMC cavity and the interferometer.

Since it was not possible to install the Faraday isolator on the former bench we had to redesign completely the SIB.

It has been required to have:

- A Faraday isolator with a degree of isolation higher than 30 dB.
- Matching of the beam on the interferometer (mismatching < 4%).
- Matching on the Reference Cavity (RFC).
- Be able to compensate for thermal effects appearing in the Faraday isolator by using telescopes.
- Be able to compensate for IMC end mirror ROC errors.

The new bench has been designed both with two optical ray tracing software (Zemax and Optocad) and with Autocad and Autodesk Inventor, for taking into account the mechanical dimensions of the components and mounts.

Zemax has been mostly used for designing the telescopes (namely the parabolic telescope and tolerancing, beam profiles, aberrations, etc.). Optocad has been used for an evaluation of the beam paths and dimension on the bench. Autocad and Inventor have been used for the mechanical design of the bench and of all the components.

2.2. Optical design

On figure 1, there is a drawing of the upper part of the new Suspended Injection Bench and on figure 2, you can find the optical layout of the SIB lower part with the reference cavity in the middle.

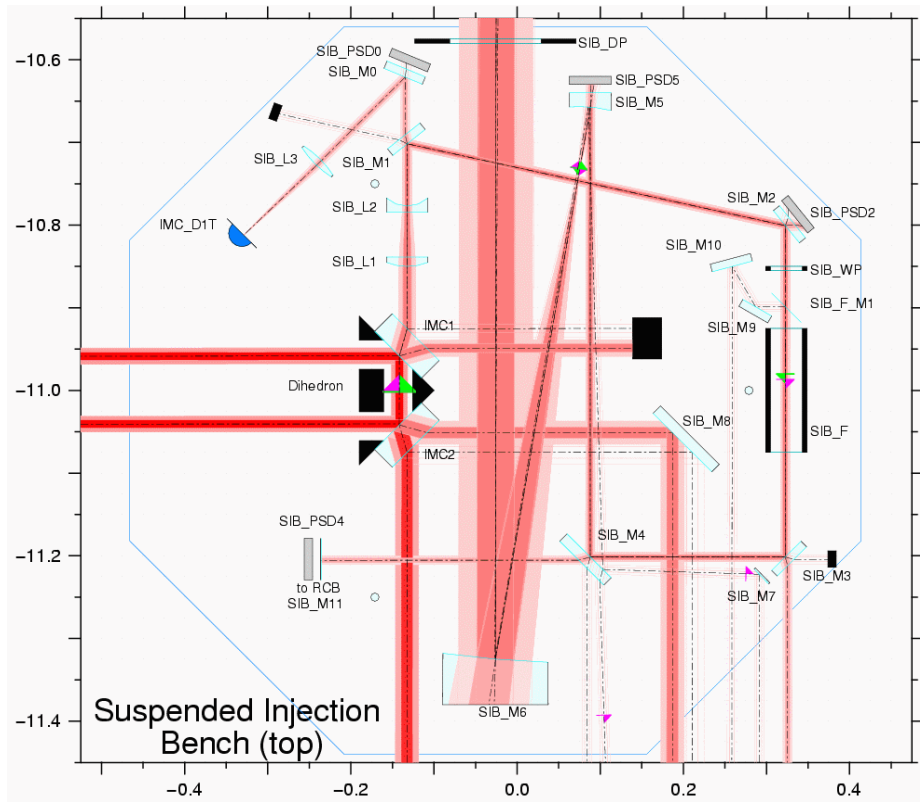


Figure 1: Layout of the new SIB (upper part) with Optocad.

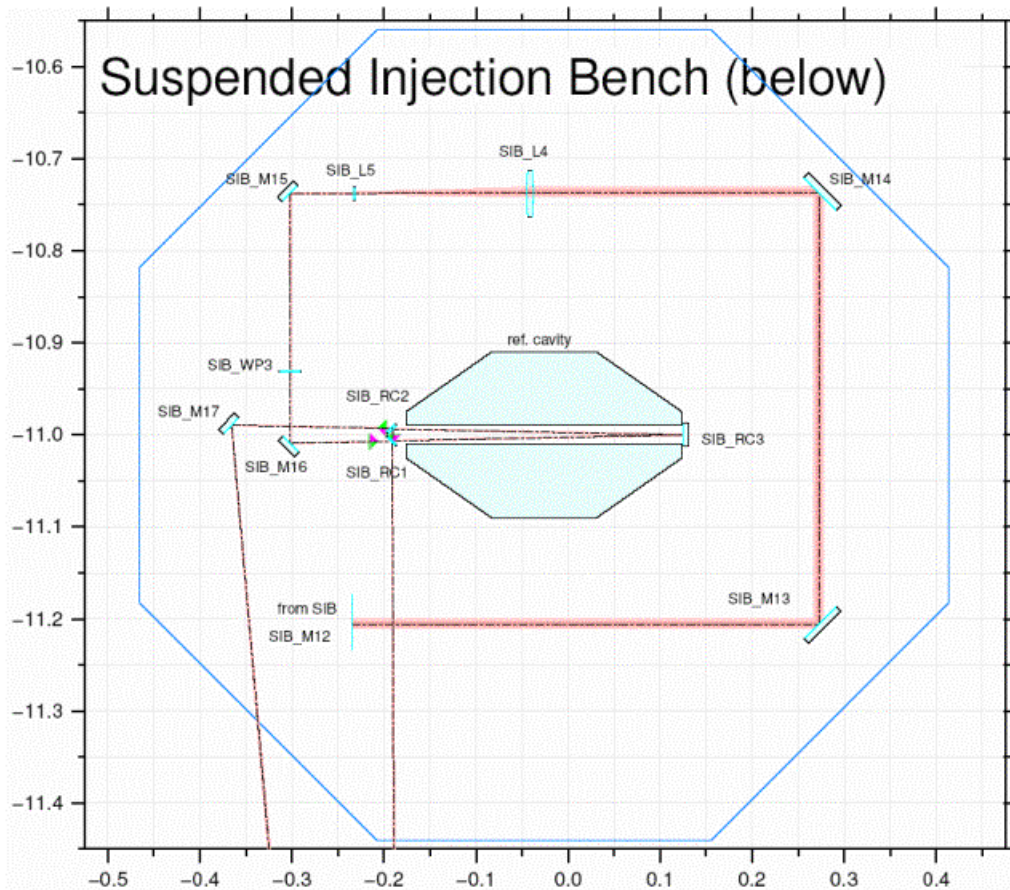


Figure 2: Layout of the new SIB (lower part) with Optocad.

Going a little bit more into the details, the laser beam coming from the laser lab is entering the Injection tower by a tilted window with AR coating on both faces. The 4.9 mm waist size beam is then coupled in the IMC cavity. The “cleaned” beam is passing through the reducing telescope T1 so that the beam waist located in the FI is 2.6 mm radius. A pick-off beam (through SIB_M1), placed where the beam is collimated, is used for the laser power stabilization loop. An EOT Faraday isolator of 20 mm clear aperture is installed between the IMC and the ITF mode matching telescope in order to avoid perturbation of IMC control loops, IMC cavity output power and to reinject light into the laser.

2.3. Mechanical design

Autocad and Inventor softwares have been used to design all the mechanics and to evaluate the space constraints of the various elements. In the Autocad design all the real dimensions of the components (mirrors, mounts, supports and actuators) have been considered. The beams are traced with a diameter of five times their waists: this provides a beam clipping smaller than 1 ppm. Mechanical drawings of the new SIB upper and lower parts can be seen on figures 3 and 4 and a top view of the SIB in the injection tower with the main beams can be seen on figure 5.

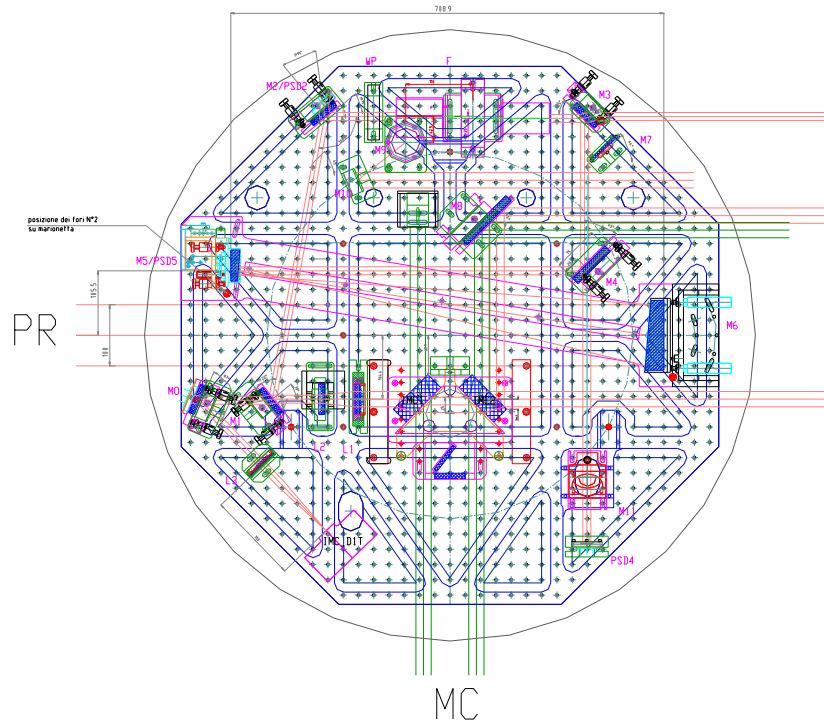


Figure 3: Mechanical scheme of the SIB (Autocad).

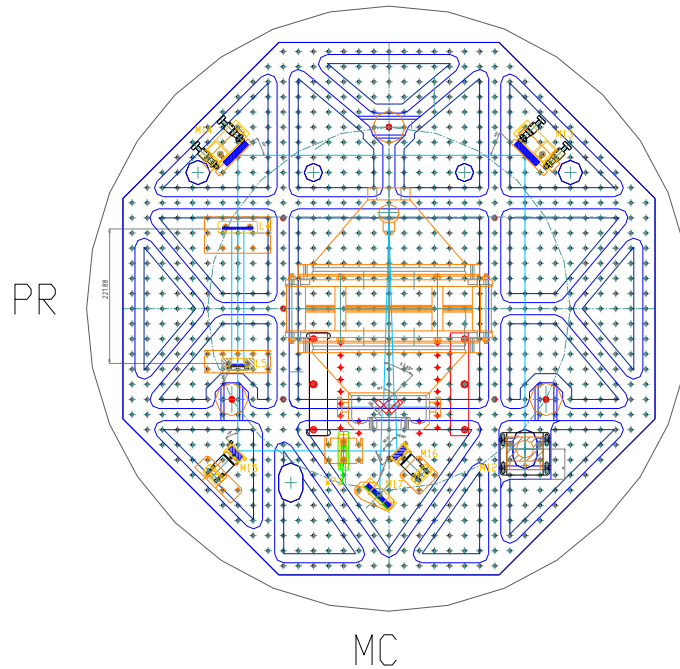


Figure 4: Mechanical scheme of the lower part of the SIB with the Reference Cavity located in the center of the bench (Autocad).

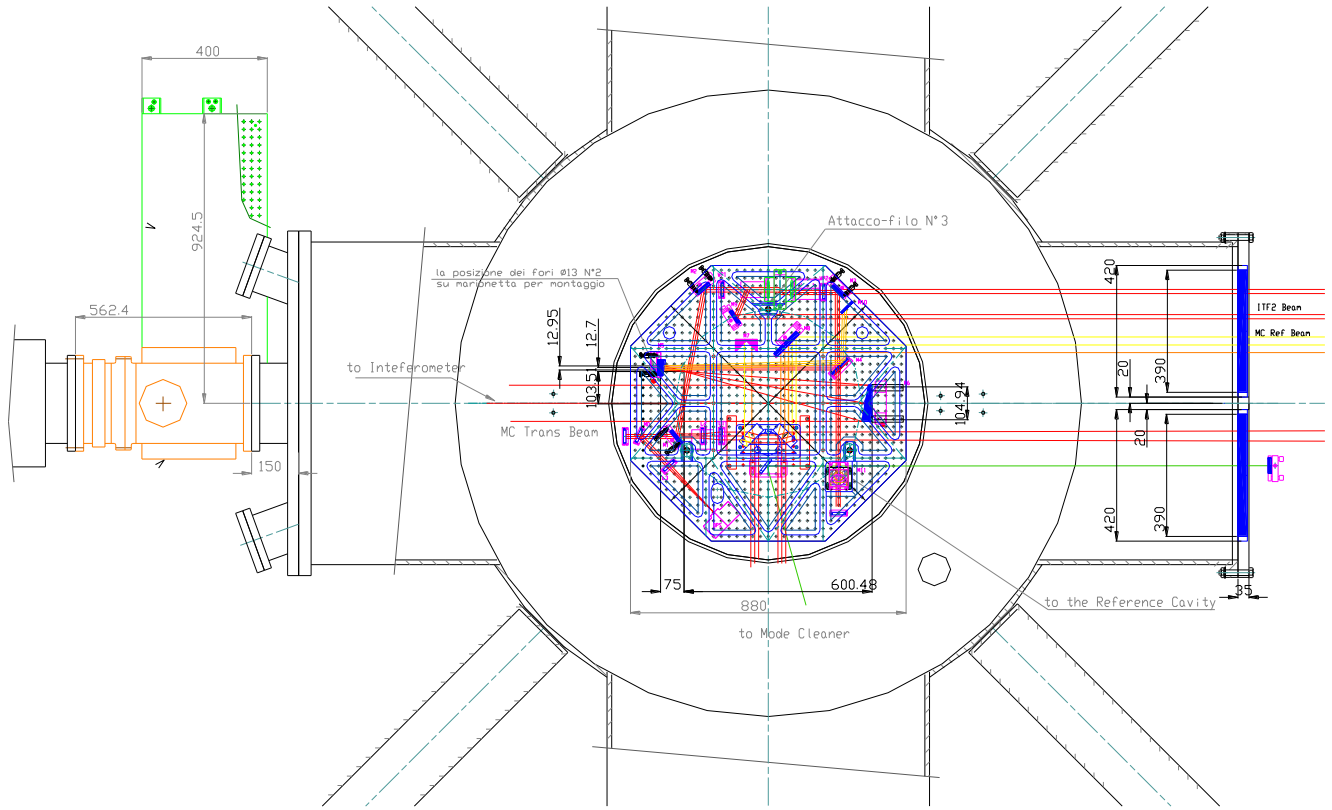


Figure 5: Scheme of the bench inside INJ tower.

In the next chapter we will focus on the parabolic telescope design.

3. Telescope trade-off analysis

During the design process, it had been shown that without reducing the size of the beam passing through the FI the diffraction effects start to be significant at a 10^{-3} of the normalized power.

Keeping all of these things in mind,, we have proposed to reduce the beam size before the FI down to a beam having the waist of less than 3 mm localized in the FI. Therefore, between the IMC and the FI a reducing telescope (T1) has to be placed which reduces the waist of the beam from 4.9 mm of the IMC to less than 3 mm inside the Faraday. The telescope after the FI (T2) which enlarges the beam to the size needed by the ITF has to be designed accordingly.

T2 should allow the optimization of the matching of the beam on the interferometer.

The following aspects are analyzed hereafter:

- 1) Design of the T1 telescope to reduce the beam size down to less than 3 mm: two possible T1 telescopes: a longer (about 250 mm) and a shorter one (about 150 mm);
- 2) Design of the T2 telescope, in different configurations:
 - a. T2 made with spherical mirrors
 - b. T2 made with parabolic mirrors¹

3.1. Refractive telescope (e.g. T1)

A refractive telescope is used for adapting the beam diameter to the Faraday clear aperture. After several simulations, it has been decided to use an afocal, made of a spherical-plane converging lens, followed by a plane-spherical diverging lens. It has to reduce the beam from 4.9 mm to 2.65 mm (reducing power of about 2). This telescope has to be short (not more than 20 cm), owing to space constraints on the bench. The use of a refractive telescope in this position is justified since, being located before the FI (with respect of the ITF), it does not reflect back to the ITF a significant amount of light.

3.1.1. T1 design

T1 is based on a classical Galilean design. Different lens combinations have been considered depending on the room available at each stage of the bench design. Over the configuration chosen 3 different telescopes based on the following combinations have been studied:

- Custom/custom lens based telescope (cons: price--, delivery time / pro: performances with respect to matching, MTF)
- Custom/Off the shelf lens based telescope (cons price-, delivery time / pro: performances with respect to matching)
- Off the shelf/Off the shelf lens based telescope (cons: performances with respect to matching/ pro: price++, delivery time++)

¹ Note that only Keplerian telescope configuration will be presented here since the Galilean one was not advisable due to the difficulty to realize a convex parabolic mirror with such a short focal length, and the extremely high cost and long delivery time of such a kind of mirror at the time the SIB has been designed.

At the end a very compact telescope with off the shelf lenses has been chosen both for space and cost issues. This compact telescope should allow us to have enough space to eventually install an Electro optical modulator in the immediate vicinity of the Faraday isolator (it was required to keep this option opened).

3.1.2. Off the shelf/off the shelf lens based telescope: our choice for the next IB

Lens 1: CVI #PLCX-50.8-67.0-UV (fused silica, F=149mm@1064nm, D=50.8mm)

Lens 2: Optosigma #012-0445 (fused silica, F=-80mm, D=50mm)

Lens Data Editor							
Surf	Type	Comment	Radius	Thickness	Glass	Semi-Diameter	Conic
OBJ	Standard		Infinity	Infinity		Infinity	0.000
1	Standard	INPUT WAIST	Infinity	200.000		0.000	U 0.000
2	Coordinat...			0.000	-	0.000	
3*	Standard	PLCX-50.8-67...	67.000	6.600	SILICA	25.400	U 0.000
4*	Standard		Infinity	60.500	V	25.000	U 0.000
5*	Standard	012-0445	Infinity	3.000	SILICA	25.000	U 0.000
6*	Standard		36.800	0.000		25.000	U 0.000
STO	Coordinat...			0.000	-	0.000	
8	Standard		Infinity	830.000		0.000	U 0.000
9	Standard		Infinity	0.000		165.437	0.000
IMA	Standard	#1 WAIST LOCA...	Infinity	-		0.000	U 0.000

Figure 6- Off-the-shelf lens based telescope Zemax lens editor.

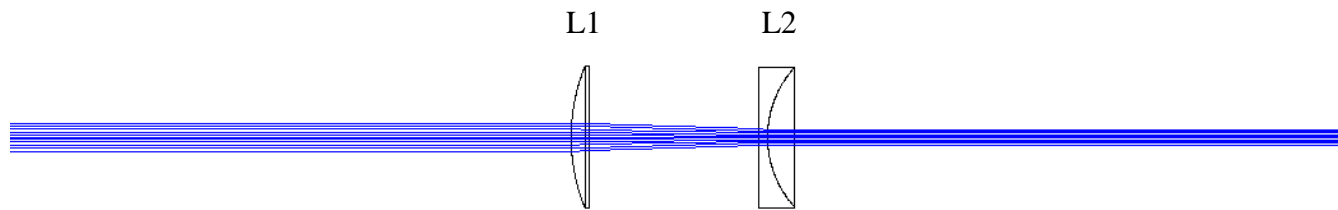


Figure 7 – Profile layout of the shortened Galilean telescope.

3.1.2.1 Performances: imaging

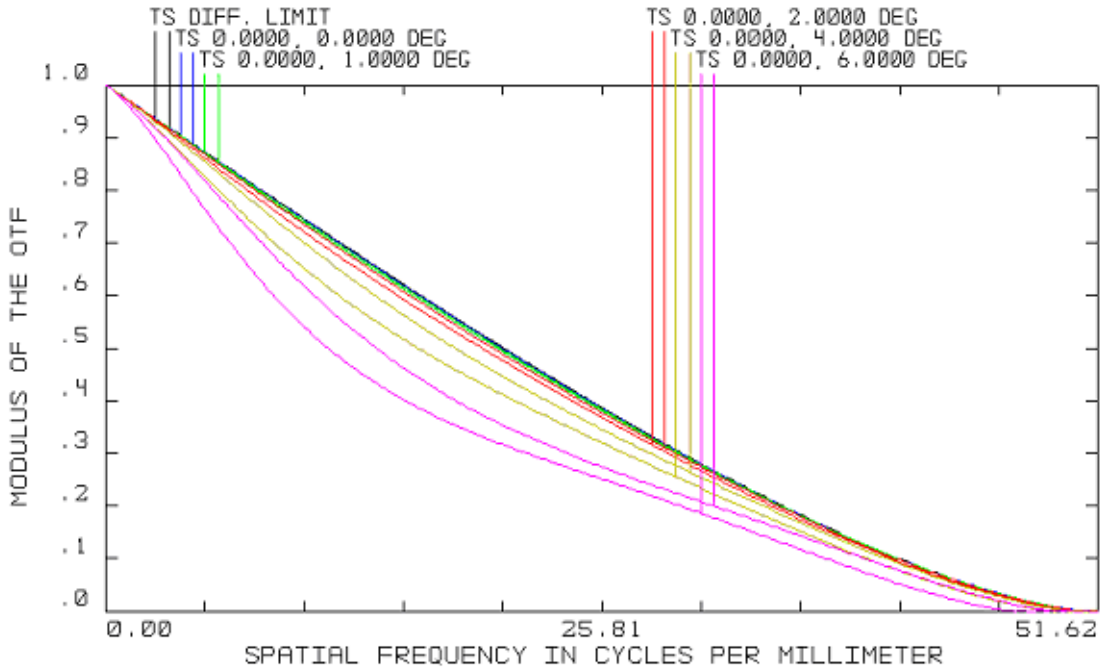


Figure 8 - MTF at 0deg, 1deg, 2deg, 4deg, 6deg with a dummy paraxial surface preceding the focus plane

Concerning the intrinsic performances of the telescope one can observe on the previous plot that for an input beam direction within $-2...+2$ deg and for a gaussian beam (5mm input waist) the proposed telescope is diffraction limited. The performances get noticeably worst for higher incident directions ($>3-4$ deg).

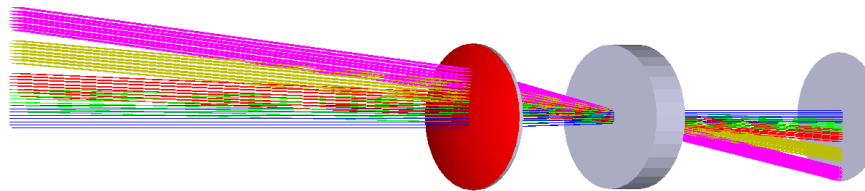


Figure 9 – Beams at various field angles impinging the first telescope lens (red surface)

3.1.2.2 Performances: gaussian optics

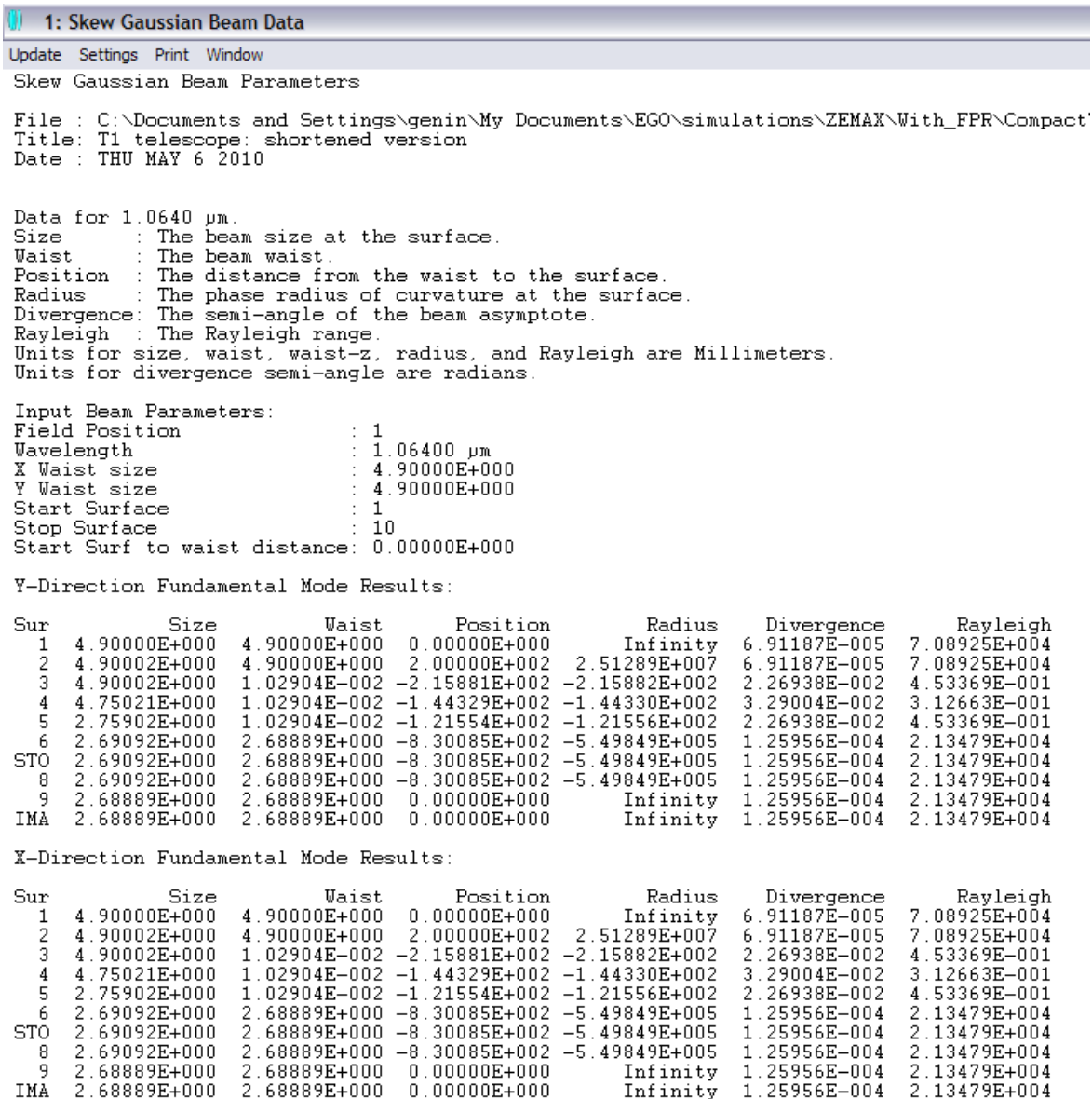


Figure 10 - Results of the physical optics propagation

Assuming that the input waist is located 200 mm before the first lens (the waist is located between the dihedron input/output mirrors), propagating a gaussian beam through the telescope leads to the results indicated above (see Figure): 2.69 mm waist size, waist location on surface#9 (830 mm after the telescope lens#2 (located in the Faraday isolator)).

We indicate below the influence of the lens separation (within a +/-0.2mm range) on both the waist position and size. By modifying the separation one can adjust the waist location (first order effect) without severely modifying its size (second order effect) as you can see on figures 6 and 7.

The waist position changes almost linearly with a slope of about -65m/mm.

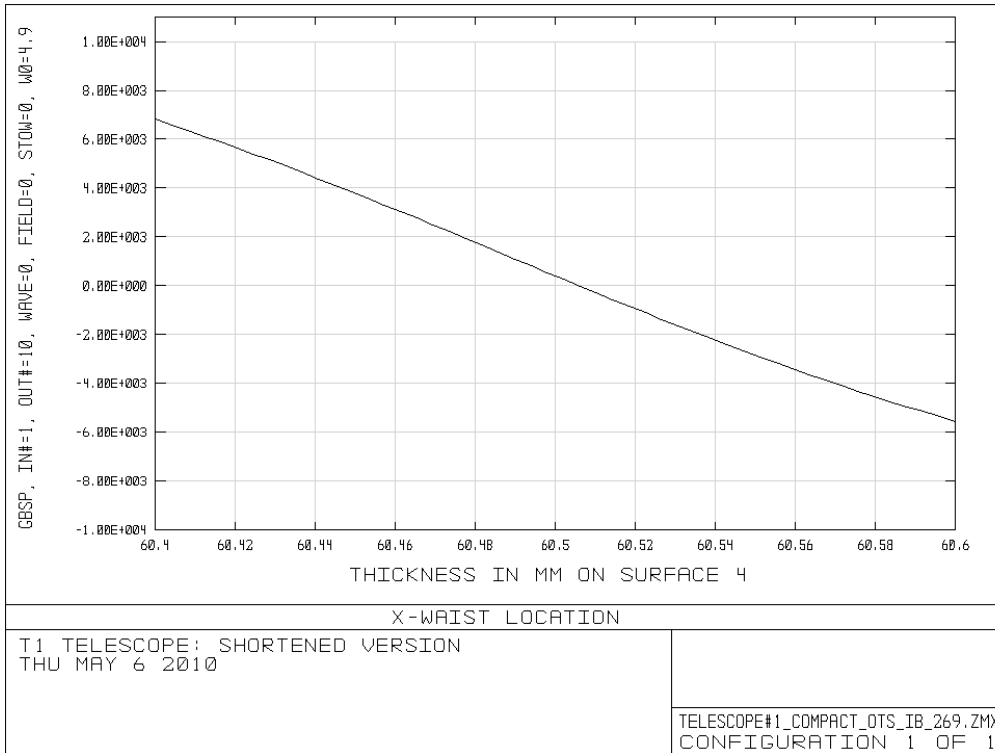


Figure 11: Waist position change after T1 telescope versus distance between L1 and L2 (SURFACE 4).

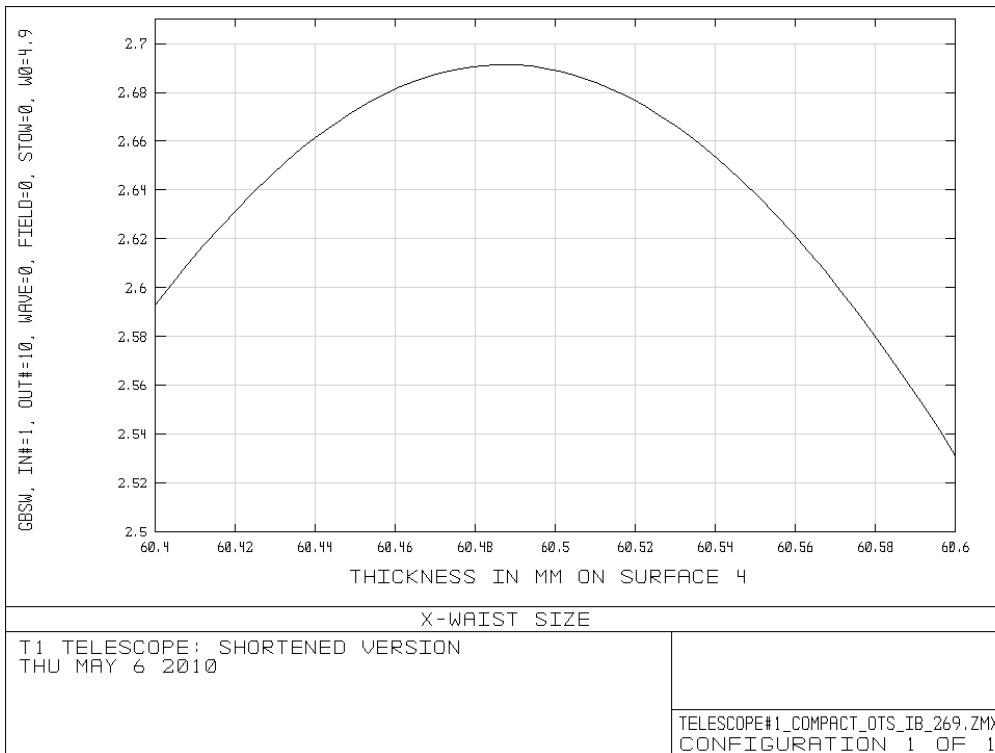


Figure 12: Waist size change after T1 telescope versus distance between L1 and L2 (SURFACE 4).

3.2. Design of the T2 telescope

For designing this telescope, we have considered 2 different configurations of the reflective telescope:

- T2 made with spherical mirrors
- T2 made with parabolic mirrors

The parameters to be considered in the design are:

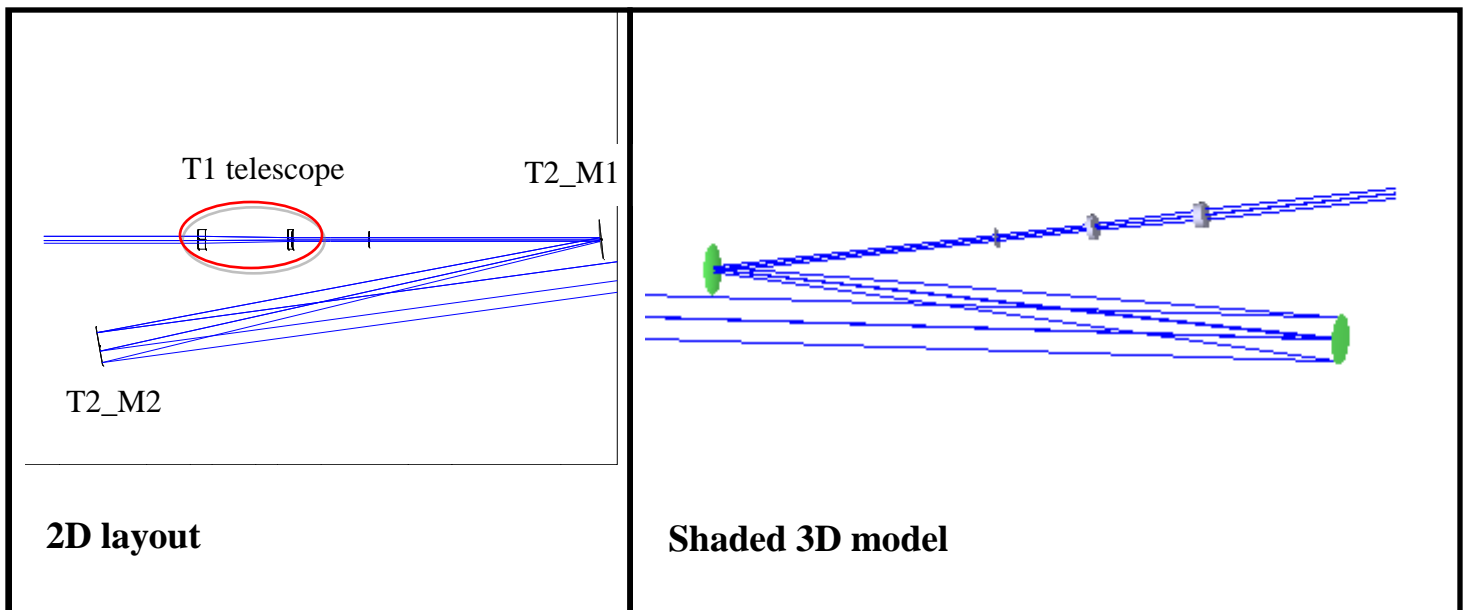
- The telescope has to be “short” (not longer than 800 mm (SIB body maximum dimension));
- Aberrations have to be avoided (in particular spherical aberrations and astigmatism);
- Sensitivity to misalignments and mismatching has to be evaluated.

In the next paragraphs, the spherical mirrors telescope will be shortly presented. Then, the chosen configuration (parabolic telescope) will be presented more in details from the simulation point of view.

3.2.1. Spherical mirrors telescope with refractive telescope T1

The first reflective telescope considered has been a telescope based on spherical mirrors

3.2.1.1 Proposed optical design





Lens Data Editor						
Edit Solves Options Help						
Surf:Type	Comment	Radius	Thickness	Class	Semi-Diameter	
OBJ*	Standard	Infinity	Infinity		0.000000	
1	Standard	INPUT WAIST	Infinity	200.000000		0.000000 U
2*	Standard	T1-LENS#1	129.428679	10.000000	BK7	12.700000 U
3*	Standard	T1-LENS#2	Infinity	107.260453		12.700000 U
4*	Standard	T2-LENS#2	Infinity	5.000000	BK7	12.700000 U
5*	Standard	T2-LENS#2	70.000000	0.000000		12.700000 U
6*	Standard	ENT APERT FI	Infinity	50.000000		20.000000 U
7	Standard	WAIST #1-FI CENTER	Infinity	50.000000		0.000000 U
8*	Standard	EXIT APERT FI	Infinity	300.000000		20.000000 U
9	Coordinate B..			0.000000	-	0.000000
ST0*	Standard	T2-FOLD MIRROR #1	190.000000	0.000000	MIRROR	25.400000 U
11	Coordinate B..			-664.868812	V	0.000000
12	Coordinate B..			0.000000	-	0.000000
13*	Standard	T2-FOLD MIRROR #2	1519.710603	0.000000	MIRROR	50.800000 U
14	Coordinate B..			5288.000000	-	0.000000
15*	Standard	FLAT POWER RECYC	Infinity	30.000000	SUPRASIL	60.000000 U
16*	Standard		Infinity	1.200000E+004		60.000000 U
17	Standard	WAIST #2-3 KM ARM	Infinity	3.000000E+006		200.000000 U
IMA	Standard		Infinity	-		200.000000 U

Lens Data Editor				
Edit Solves Options Help				
Surf:Type	Par 2 (unused)	Par 3 (unused)		
OBJ*	Standard			
1	Standard			
2*	Standard			
3*	Standard			
4*	Standard			
5*	Standard			
6*	Standard			
7	Standard			
8*	Standard			
9	Coordinate B..	0.000000	6.000000	
ST0*	Standard			
11	Coordinate B..	0.000000	6.000000	P
12	Coordinate B..	0.000000	-2.122770	V
13*	Standard			
14	Coordinate B..	0.000000	-2.122770	P
15*	Standard			
16*	Standard			
17	Standard			
IMA	Standard			

The incidence angle on the first mirror is 6 deg. (horizontal plane)
 Depending on potential obscuration problems in front of M5 mirror, a higher incidence angle may be chosen. The incidence angle on the second mirror should be then re-tuned in order to maintain the astigmatism-free condition (this condition requires a 2.88 deg incidence angle).

3.2.1.2 Gaussian optics

```

Input Beam Parameters:
Field Position          : 1
Wavelength              : 1.06400 µm
X Waist size           : 4.90000E+000
Y Waist size           : 4.90000E+000
Start Surface          : 1
Stop Surface           : 18
Start Surf to waist distance: 0.00000E+000

Y-Direction Fundamental Mode Results:

Sur      Size      Waist      Position      Radius      Divergence      Rayleigh
1  4.90000E+000  4.90000E+000  0.00000E+000  Infinity  6.91187E-005  7.08925E+004
2  4.90002E+000  1.76433E-002  -3.84689E+002  -3.84694E+002  1.27369E-002  1.38514E+000
3  4.77264E+000  1.76433E-002  -2.48625E+002  -2.48628E+002  1.91937E-002  9.19112E-001
4  2.71369E+000  1.76433E-002  -2.13042E+002  -2.13051E+002  1.27369E-002  1.38514E+000
5  2.65001E+000  2.65000E+000  -5.00000E+001  -8.59869E+006  1.27804E-004  2.07348E+004
6  2.65001E+000  2.65000E+000  -5.00000E+001  -8.59869E+006  1.27804E-004  2.07348E+004
7  2.65000E+000  2.65000E+000  1.06542E-006  Infinity  1.27804E-004  2.07348E+004
8  2.65001E+000  2.65000E+000  5.00000E+001  8.59869E+006  1.27804E-004  2.07348E+004
9  2.65038E+000  2.65000E+000  3.50000E+002  1.22873E+006  1.27804E-004  2.07348E+004
STO 2.67028E+000  1.20482E-002  -9.42827E+001  -9.42846E+001  2.81033E-002  4.28597E-001
11  2.67028E+000  1.20482E-002  -9.42827E+001  -9.42846E+001  2.81033E-002  4.28597E-001
12  2.13395E+001  1.20482E-002  -7.59126E+002  -7.59126E+002  2.81033E-002  4.28597E-001
13  2.13595E+001  2.13378E+001  -1.73087E+004  -1.04429E+008  1.58724E-005  1.34433E+006
14  2.13595E+001  2.13378E+001  -1.73087E+004  -1.04429E+008  1.58724E-005  1.34433E+006
15  2.13386E+001  2.13378E+001  -1.74304E+004  -2.18020E+008  1.09463E-005  1.94938E+006
16  2.13386E+001  2.13378E+001  -1.20000E+004  -1.50614E+008  1.58724E-005  1.34433E+006
17  2.13378E+001  2.13378E+001  4.32647E-005  Infinity  1.58724E-005  1.34433E+006
IMA 5.21795E+001  2.13378E+001  3.00000E+006  3.60241E+006  1.58724E-005  1.34433E+006

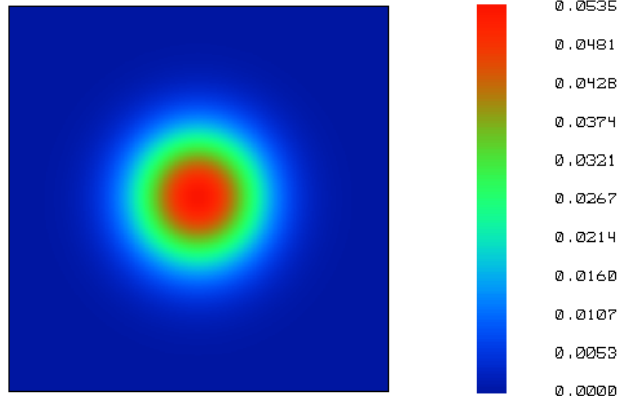
X-Direction Fundamental Mode Results:

Sur      Size      Waist      Position      Radius      Divergence      Rayleigh
1  4.90000E+000  4.90000E+000  0.00000E+000  Infinity  6.91187E-005  7.08925E+004
2  4.90002E+000  1.76433E-002  -3.84689E+002  -3.84694E+002  1.27369E-002  1.38514E+000
3  4.77264E+000  1.76433E-002  -2.48625E+002  -2.48628E+002  1.91937E-002  9.19112E-001
4  2.71369E+000  1.76433E-002  -2.13042E+002  -2.13051E+002  1.27369E-002  1.38514E+000
5  2.65001E+000  2.65000E+000  -5.00000E+001  -8.59869E+006  1.27804E-004  2.07348E+004
6  2.65001E+000  2.65000E+000  -5.00000E+001  -8.59869E+006  1.27804E-004  2.07348E+004
7  2.65000E+000  2.65000E+000  1.06542E-006  Infinity  1.27804E-004  2.07348E+004
8  2.65001E+000  2.65000E+000  5.00000E+001  8.59869E+006  1.27804E-004  2.07348E+004
9  2.65038E+000  2.65000E+000  3.50000E+002  1.22873E+006  1.27804E-004  2.07348E+004
STO 2.65038E+000  1.22298E-002  -9.57039E+001  -9.57060E+001  2.76861E-002  4.41616E-001
11  2.65038E+000  1.22298E-002  -9.57039E+001  -9.57060E+001  2.76861E-002  4.41616E-001
12  2.10620E+001  1.22298E-002  -7.60547E+002  -7.60547E+002  2.76861E-002  4.41616E-001
13  2.10620E+001  2.10602E+001  -1.73087E+004  -9.91001E+007  1.60816E-005  1.30958E+006
14  2.10620E+001  2.10602E+001  -1.73087E+004  -9.91001E+007  1.60816E-005  1.30958E+006
15  2.10610E+001  2.10602E+001  -1.74304E+004  -2.06894E+008  1.10905E-005  1.89893E+006
16  2.10610E+001  2.10602E+001  -1.20000E+004  -1.42928E+008  1.60816E-005  1.30958E+006
17  2.10602E+001  2.10602E+001  8.81934E-005  Infinity  1.60816E-005  1.30958E+006
IMA 5.26413E+001  2.10602E+001  3.00000E+006  3.57166E+006  1.60816E-005  1.30958E+006
  
```

One can note from the previous table and figure 13 that the astigmatism is almost cancelled at the input of the interferometer (surf. 17). Nevertheless, the beam shape after 3 kms of propagation is not perfect and a bit astigmatic as you can see on figure 14. This is why we also considered the possibility to use parabolic off-axis mirror that should allow having a perfect beam shape both at the input of the Fabry-Perot cavity and after 3kms of propagation.



Modeled beam shape @ 17.288m (input mirror location)

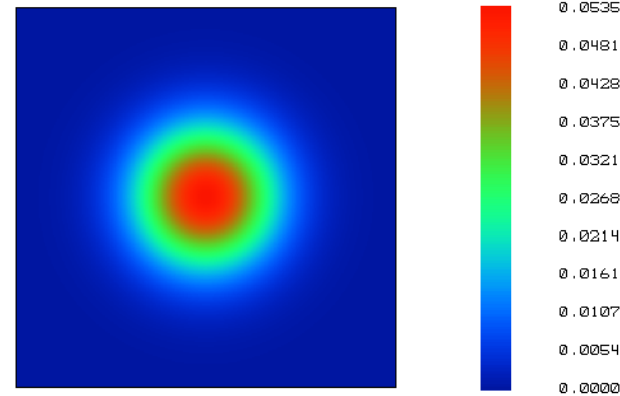


TOTAL IRRADIANCE SURFACE 17 WAIST #2-3 KM ARM

```

MON NOV 8 14:33:46 2004
WAVELENGTH 1.0640 #M AT 0.0000, 0.0000 DEG
DISPLAY X WIDTH = 8.5955E+001, Y HEIGHT = 8.7097E+001 MILLIMETERS
PEAK IRRADIANCE = 5.3462E-002 WATTS/MILLIMETERS^2, TOTAL POWER = 3.7711E+001 WATTS
X PILOT: SIZE= 2.1060E+001, WAIST= 2.1060E+001, POS= +9.0413E-001, RAYLEIGH= 1.3096E+006
Y PILOT: SIZE= 2.1338E+001, WAIST= 2.1338E+001, POS= +9.8316E-001, RAYLEIGH= 1.3443E+006
  
```

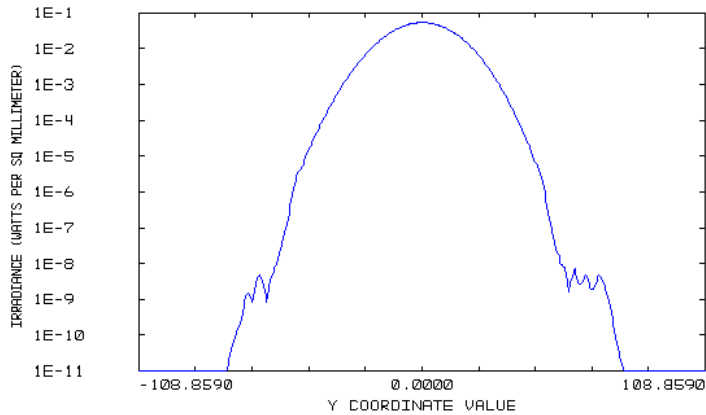
Ideal (aberration-free) beam @ 17.288m (input mirror location)



TOTAL IRRADIANCE SURFACE 17 WAIST #2-3 KM ARM

```

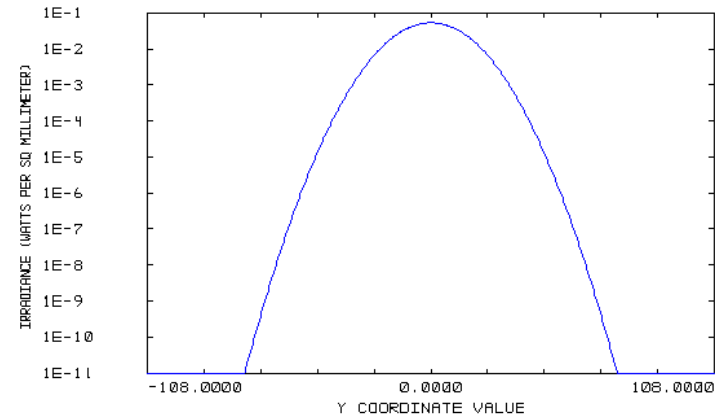
MON NOV 8 14:44:10 2004
WAVELENGTH 1.0640 #M AT 0.0000, 0.0000 DEG
DISPLAY X WIDTH = 8.0000E+001, Y HEIGHT = 8.0000E+001 MILLIMETERS
PEAK IRRADIANCE = 5.3500E-002 WATTS/MILLIMETERS^2, TOTAL POWER = 3.7758E+001 WATTS
X PILOT: SIZE= 2.1200E+001, WAIST= 2.1200E+001, POS= +0.0000E+000, RAYLEIGH= 1.3270E+006
Y PILOT: SIZE= 2.1200E+001, WAIST= 2.1200E+001, POS= +0.0000E+000, RAYLEIGH= 1.3270E+006
  
```



IRRADIANCE Y-CROSS SECTION SURFACE 17 WAIST #2-3 KM ARM

```

MON NOV 8 14:34:5 2004
WAVELENGTH 1.0640 #M AT 0.0000, 0.0000 DEG
CENTER X = 0.0000E+000
PEAK IRRADIANCE = 5.3473E-002 WATTS/MILLIMETERS^2, TOTAL POWER = 3.7715E+001 WATTS
Y PILOT: SIZE= 2.1060E+001, WAIST= 2.1060E+001, POS= +5.4063E-001, RAYLEIGH= 1.3096E+006
Y PILOT: SIZE= 2.1338E+001, WAIST= 2.1338E+001, POS= +5.9839E-001, RAYLEIGH= 1.3443E+006
  
```



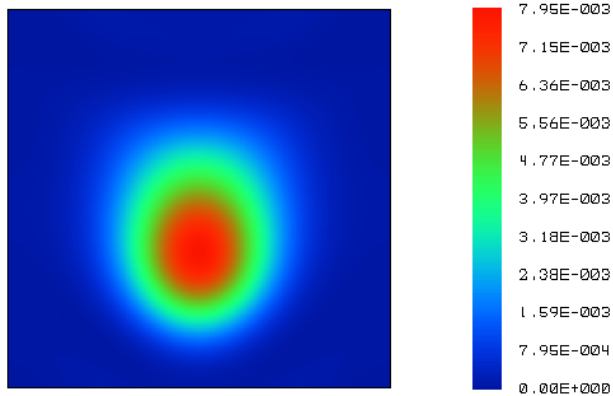
IRRADIANCE Y-CROSS SECTION SURFACE 17 WAIST #2-3 KM ARM

```

MON NOV 8 14:44:17 2004
WAVELENGTH 1.0640 #M AT 0.0000, 0.0000 DEG
CENTER X = 0.0000E+000
PEAK IRRADIANCE = 5.3500E-002 WATTS/MILLIMETERS^2, TOTAL POWER = 3.7770E+001 WATTS
Y PILOT: SIZE= 2.1200E+001, WAIST= 2.1200E+001, POS= +0.0000E+000, RAYLEIGH= 1.3270E+006
Y PILOT: SIZE= 2.1200E+001, WAIST= 2.1200E+001, POS= +0.0000E+000, RAYLEIGH= 1.3270E+006
  
```

Figure 13: Comparison of the beam size on Fabry-Perot cavities input mirrors at the output of T2 telescope respect to a perfect Gaussian beam.

Modeled beam shape @ 3km

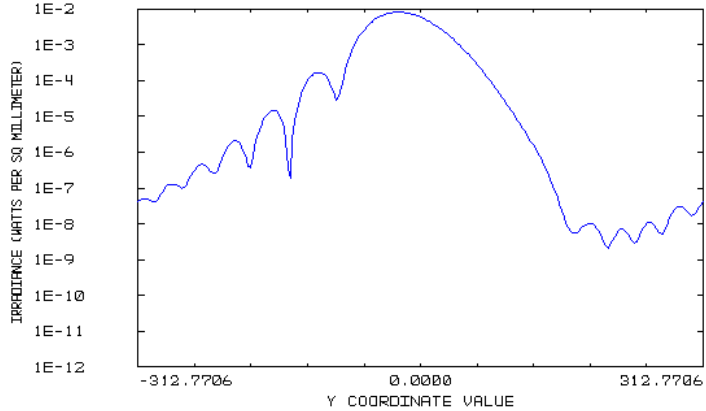


TOTAL IRRADIANCE SURFACE 18

```

MON NOV 8 14:33:47 2004
WAVELENGTH 1.0640 #M AT 0.0000, 0.0000 DEG
DISPLAY X WIDTH = 1.8767E+002, Y HEIGHT = 1.8569E+002 MILLIMETERS
PEAK IRRADIANCE = 7.9451E-003 WATTS/MILLIMETERS^2, TOTAL POWER = 3.7778E+001 WATTS
X PILOT: SIZE= 5.2179E+001, WAIST= 2.1332E+001, PDS= +2.9992E+006, RAYLEIGH= 1.2435E+006
Y PILOT: SIZE= 5.2179E+001, WAIST= 2.1332E+001, PDS= +2.9992E+006, RAYLEIGH= 1.2435E+006

```



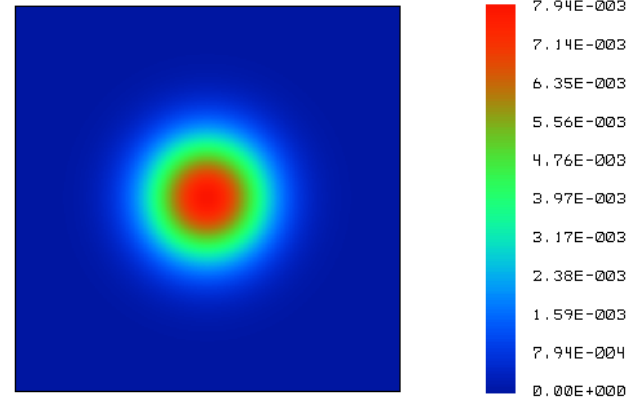
IRRADIANCE Y-CROSS SECTION SURFACE 18

```

MON NOV 8 14:33:59 2004
WAVELENGTH 1.0640 #M AT 0.0000, 0.0000 DEG
CENTER, X = 0.0000E+000
PEAK IRRADIANCE = 8.1011E-003 WATTS/MILLIMETERS^2, TOTAL POWER = 3.7715E+001 WATTS
X PILOT: SIZE= 5.2641E+001, WAIST= 2.1060E+001, PDS= +3.0000E+006, RAYLEIGH= 1.3095E+006
Y PILOT: SIZE= 5.2179E+001, WAIST= 2.1338E+001, PDS= +3.0000E+006, RAYLEIGH= 1.3443E+006

```

Ideal (aberration-free) beam @ 3km

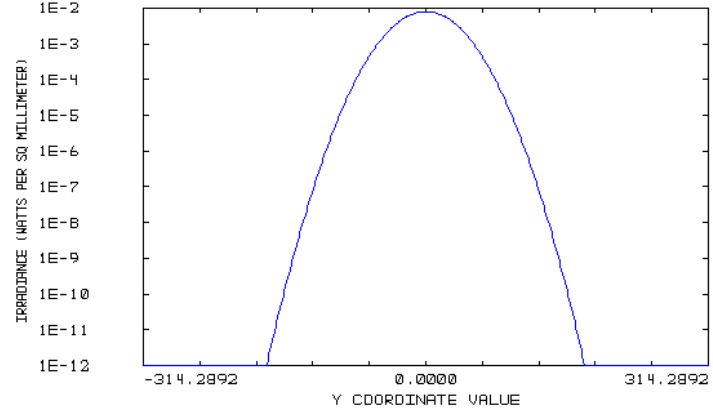


TOTAL IRRADIANCE SURFACE 18

```

MON NOV 8 14:52:15 2004
WAVELENGTH 1.0640 #M AT 0.0000, 0.0000 DEG
DISPLAY X WIDTH = 2.3347E+002, Y HEIGHT = 2.3347E+002 MILLIMETERS
PEAK IRRADIANCE = 7.9369E-003 WATTS/MILLIMETERS^2, TOTAL POWER = 3.4241E+001 WATTS
X PILOT: SIZE= 5.2406E+001, WAIST= 2.1200E+001, PDS= +3.0000E+006, RAYLEIGH= 1.3270E+006
Y PILOT: SIZE= 5.2406E+001, WAIST= 2.1200E+001, PDS= +3.0000E+006, RAYLEIGH= 1.3270E+006

```



IRRADIANCE Y-CROSS SECTION SURFACE 18

```

MON NOV 8 14:52:26 2004
WAVELENGTH 1.0640 #M AT 0.0000, 0.0000 DEG
CENTER, X = 0.0000E+000
PEAK IRRADIANCE = 7.9369E-003 WATTS/MILLIMETERS^2, TOTAL POWER = 3.4240E+001 WATTS
X PILOT: SIZE= 5.2406E+001, WAIST= 2.1200E+001, PDS= +3.0000E+006, RAYLEIGH= 1.3270E+006
Y PILOT: SIZE= 5.2406E+001, WAIST= 2.1200E+001, PDS= +3.0000E+006, RAYLEIGH= 1.3270E+006

```

Figure 14: Comparison of the beam size after 3kms of propagation of the T2 telescope output beam respect to a perfect Gaussian beam.

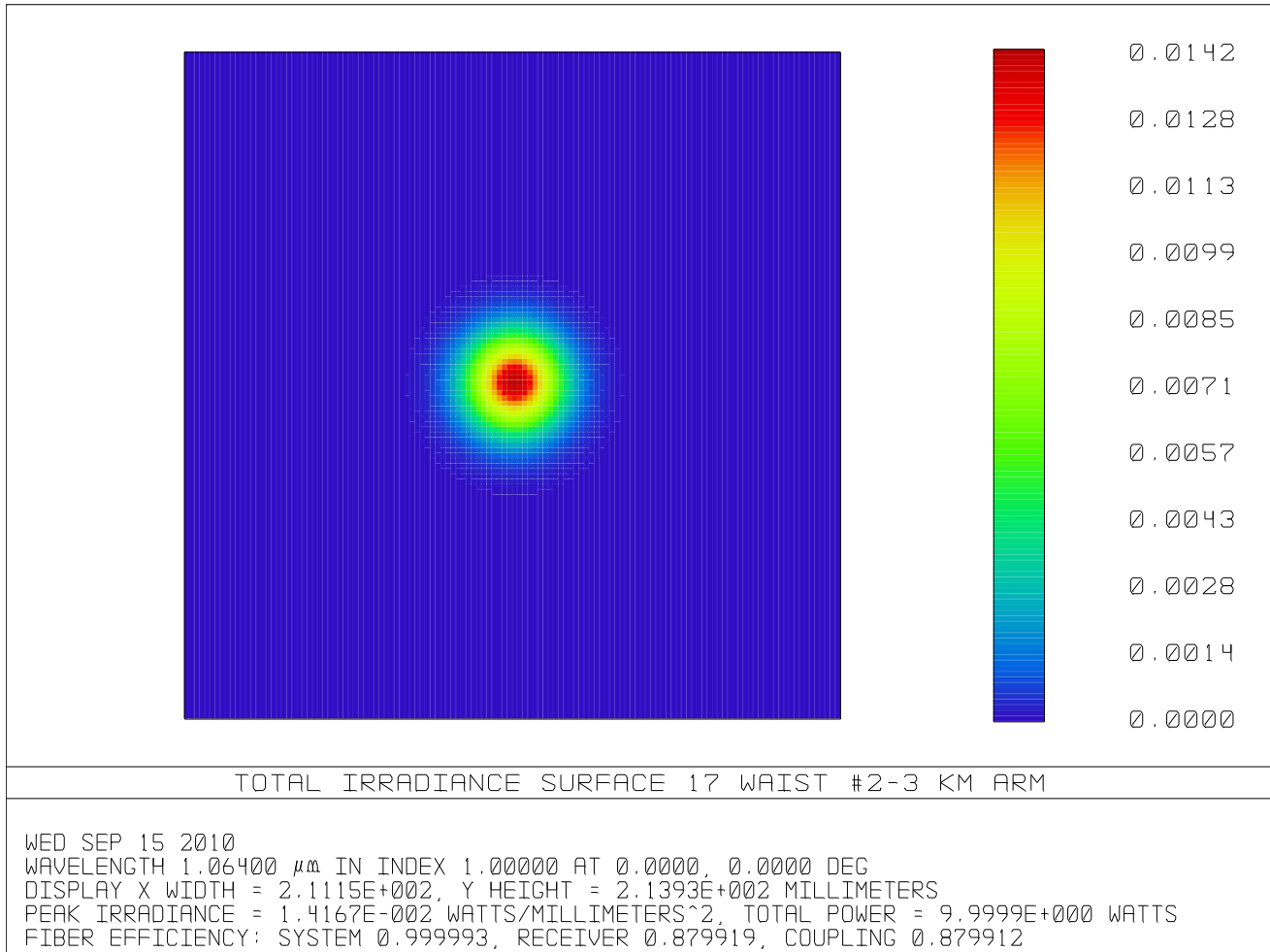


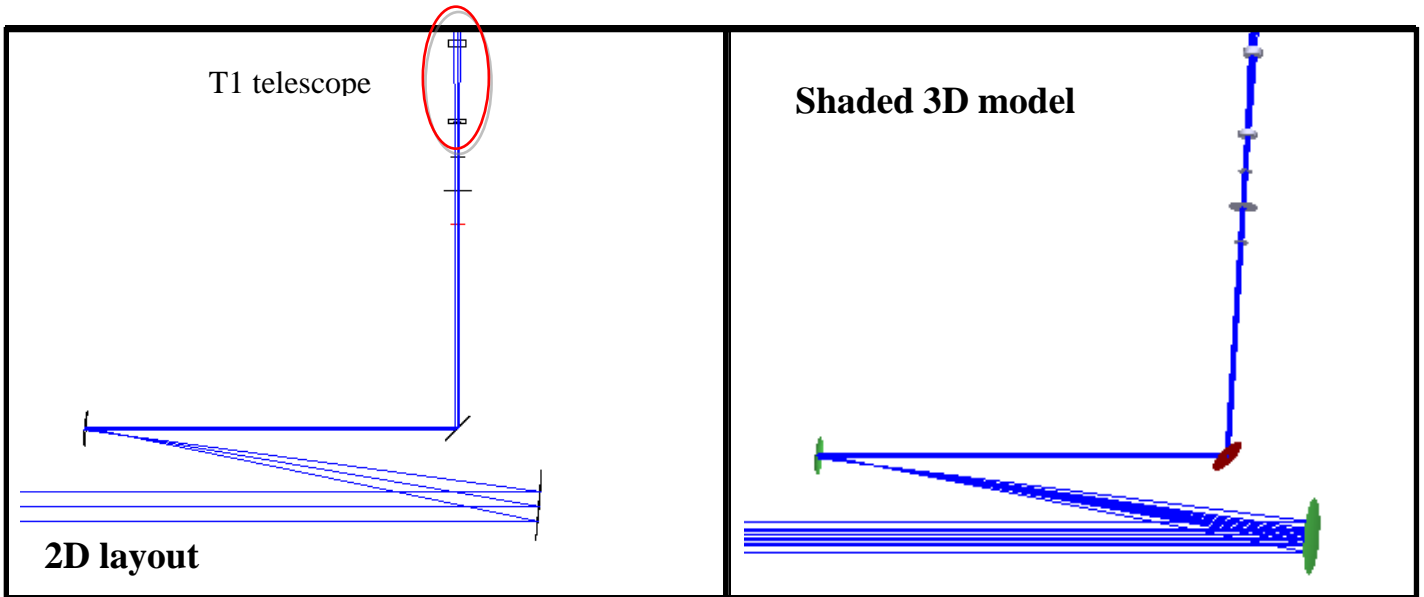
Figure 15: Beam shape at the ITF input and computation of matching on the Fabry-Perot cavities.

On figure 15, we have computed with Zemax the coupling efficiency of the beam at the output of the spherical T2 telescope. We used the fiber coupling tool provided in Zemax in order to estimate the coupling. In this case, we can see that the best matching obtained is about 88 % (considering that the cavity mode size is 20.6 mm).

3.2.2. Parabolic off-axis mirrors telescope (simulation with T1)

In this section we present the parabolic telescope design and the results obtained.

3.2.2.1 Proposed optical design



Surf:Type	Comment	Radius	Thickness	Class	Semi-Diameter	Conic
OBJ	Standard	Infinity	Infinity		0.000000	0.000000
1	Standard	INPUT WAIST	200.000000		0.000000	U 0.000000
2*	Standard	T1-LENS#1	129.428679	BK7	12.700000	U 0.000000
3*	Standard	T1-LENS#2	Infinity		12.700000	U 0.000000
4*	Standard	T2-LENS#2	Infinity	BK7	12.700000	U 0.000000
5*	Standard	T2-LENS#2	70.000000		12.700000	U 0.000000
6*	Standard	ENT APERT FI	Infinity		20.000000	U 0.000000
7	Standard	WAIST #1-FI CENTER	Infinity		20.000000	U 0.000000
8*	Standard	EXIT APERT FI	Infinity		20.000000	U 0.000000
9	Coordinate B..		0.000000	-	0.000000	
10*	Standard		Infinity	MIRROR	25.400000	U 0.000000
11	Coordinate B..		-550.000000	-	0.000000	
12	Coordinate B..		0.000000	-	0.000000	
ST0*	Standard	T2-PAR MIRROR #1	150.000000	MIRROR	25.400000	U -1.000000
14	Coordinate B..		675.014815	-	0.000000	
15	Coordinate B..		0.000000	-	0.000000	
16*	Standard	T2-PAR MIRROR #2	-1200.000000	MIRROR	80.000000	U -1.000000
17	Coordinate B..		-5288.000000	-	0.000000	
18*	Standard	FLAT POWER RECYCL..	Infinity	SUPRASIL	80.000000	U 0.000000
19*	Standard	CAVITY INPUT	Infinity		100.000000	U 0.000000
20	Standard	#2 WAIST/3 KM ARM	Infinity		0.000000	U 0.000000
IMA	Standard	CAVITY END MIRROR	Infinity		0.000000	U 0.000000



Surf	Type	Par 1 (unused)	Par 2 (unused)	Par 3 (unused)	Par 4 (unused)
OBJ	Standard				
1	Standard				
2*	Standard				
3*	Standard				
4*	Standard				
5*	Standard				
6*	Standard				
7	Standard				
8*	Standard				
9	Coordinate B..	0.000000	0.000000	0.000000	45.000000
10*	Standard				
11	Coordinate B..	0.000000	0.000000	0.000000	45.000000
12	Coordinate B..	-12.700000	0.000000	0.000000	-1.106060E-003
ST0*	Standard				
14	Coordinate B..	0.000000	0.000000	0.000000	-1.106060E-003
15	Coordinate B..	0.000000	0.000000	0.000000	1.029505E-004
16*	Standard				
17	Coordinate B..	-101.584200	0.000000	0.000000	1.029505E-004
18*	Standard				
19*	Standard				
20	Standard				
IMA	Standard				

The T1-telescope is based on an almost-afocal group. This telescope aims to adapt the waist size at the output of the mode cleaner (4.9 mm) to a size more compatible with the Faraday isolator clear aperture (2.65 mm).

The T2-telescope is based on a FL-75/FL-600 combination of off-axis parabolic mirrors implemented in an almost afocal configuration (x8 beam expansion ratio which produces a 21.2 mm waist at the input arm cavity).

The incidence angles on M5 and M6 mirrors are chosen in order to eliminate the residual astigmatism.



3.2.2.2 Gaussian optics

Results obtain by using the gaussian beam propagator:

Input Beam Parameters:

```

Field Position      : 1
Wavelength         : 1.06400 µm
X Waist size       : 4.90000E+000
Y Waist size       : 4.90000E+000
Start Surface      : 1
Stop Surface       : 21
Start Surf to waist distance: 0.00000E+000

```

Y-Direction Fundamental Mode Results:

Sur	Size	Waist	Position	Radius	Divergence	Rayleigh
1	4.90000E+000	4.90000E+000	0.00000E+000	Infinity	6.91187E-005	7.08925E+004
2	4.90002E+000	1.76433E-002	-3.84689E+002	-3.84694E+002	1.27369E-002	1.38514E+000
3	4.77264E+000	1.76433E-002	-2.48625E+002	-2.48628E+002	1.91937E-002	9.19112E-001
4	2.71369E+000	1.76433E-002	-2.13042E+002	-2.13051E+002	1.27369E-002	1.38514E+000
5	2.65001E+000	2.65000E+000	-5.00000E+001	-8.59869E+006	1.27804E-004	2.07348E+004
6	2.65000E+000	2.65000E+000	1.06542E-006	Infinity	1.27804E-004	2.07348E+004
7	2.65001E+000	2.65000E+000	5.00000E+001	8.59869E+006	1.27804E-004	2.07348E+004
8	2.65003E+000	2.65000E+000	1.00000E+002	4.29942E+006	1.27804E-004	2.07348E+004
9	2.65049E+000	2.65000E+000	4.00000E+002	1.07523E+006	1.27804E-004	2.07348E+004
10	2.65049E+000	2.65000E+000	-4.00000E+002	-1.07523E+006	1.27804E-004	2.07348E+004
11	2.65049E+000	2.65000E+000	-4.00000E+002	-1.07523E+006	1.27804E-004	2.07348E+004
12	2.65278E+000	2.65000E+000	-9.50000E+002	-4.53510E+005	1.27804E-004	2.07348E+004
ST0	2.65278E+000	9.64550E-003	-7.55493E+001	-7.55503E+001	3.50985E-002	2.74699E-001
14	2.67192E+000	9.64550E-003	-7.60945E+001	-7.60955E+001	3.50985E-002	2.74699E-001
15	2.13721E+001	9.64550E-003	6.08668E+002	6.08668E+002	3.50985E-002	2.74699E-001
16	2.12189E+001	2.12171E+001	1.73044E+004	1.02113E+008	1.59627E-005	1.32917E+006
17	2.12189E+001	2.12171E+001	1.73087E+004	1.02087E+008	1.59627E-005	1.32917E+006
18	2.12180E+001	2.12171E+001	1.74304E+004	2.13130E+008	1.10085E-005	1.92734E+006
19	2.12180E+001	2.12171E+001	1.20000E+004	1.47237E+008	1.59627E-005	1.32917E+006
20	2.12171E+001	2.12171E+001	8.04862E-003	Infinity	1.59627E-005	1.32917E+006
IMA	5.23777E+001	2.12171E+001	-3.00000E+006	-3.58890E+006	1.59627E-005	1.32917E+006

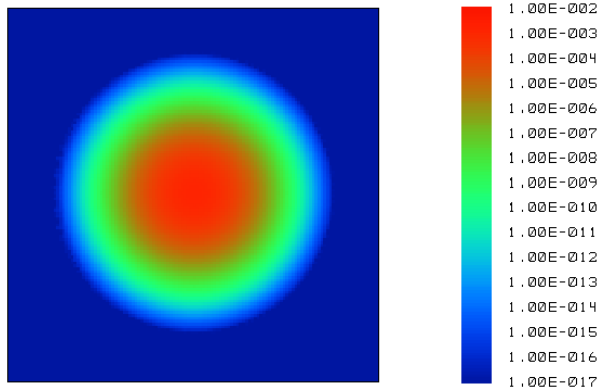
X-Direction Fundamental Mode Results:

Sur	Size	Waist	Position	Radius	Divergence	Rayleigh
1	4.90000E+000	4.90000E+000	0.00000E+000	Infinity	6.91187E-005	7.08925E+004
2	4.90002E+000	1.76433E-002	-3.84689E+002	-3.84694E+002	1.27369E-002	1.38514E+000
3	4.77264E+000	1.76433E-002	-2.48625E+002	-2.48628E+002	1.91937E-002	9.19112E-001
4	2.71369E+000	1.76433E-002	-2.13042E+002	-2.13051E+002	1.27369E-002	1.38514E+000
5	2.65001E+000	2.65000E+000	-5.00000E+001	-8.59869E+006	1.27804E-004	2.07348E+004
6	2.65000E+000	2.65000E+000	1.06542E-006	Infinity	1.27804E-004	2.07348E+004
7	2.65001E+000	2.65000E+000	5.00000E+001	8.59869E+006	1.27804E-004	2.07348E+004
8	2.65003E+000	2.65000E+000	1.00000E+002	4.29942E+006	1.27804E-004	2.07348E+004
9	2.65049E+000	2.65000E+000	4.00000E+002	1.07523E+006	1.27804E-004	2.07348E+004
10	3.74836E+000	2.65000E+000	-4.00000E+002	-1.07523E+006	1.27804E-004	2.07348E+004
11	3.74836E+000	2.65000E+000	-4.00000E+002	-1.07523E+006	1.27804E-004	2.07348E+004
12	2.65278E+000	2.65000E+000	-9.50000E+002	-4.53510E+005	1.27804E-004	2.07348E+004
ST0	2.66227E+000	9.64546E-003	-7.55491E+001	-7.55501E+001	3.50986E-002	2.74697E-001
14	2.68148E+000	9.64546E-003	-7.60942E+001	-7.60952E+001	3.50986E-002	2.74697E-001
15	2.14487E+001	9.64546E-003	6.08668E+002	6.08668E+002	3.50986E-002	2.74697E-001
16	2.12949E+001	2.12172E+001	1.73044E+004	1.02114E+008	1.59626E-005	1.32918E+006
17	2.12949E+001	2.12172E+001	1.73087E+004	1.02089E+008	1.59626E-005	1.32918E+006
18	2.12181E+001	2.12172E+001	1.74304E+004	2.13133E+008	1.10085E-005	1.92735E+006
19	2.12181E+001	2.12172E+001	1.20000E+004	1.47239E+008	1.59626E-005	1.32918E+006
20	2.12172E+001	2.12172E+001	3.72123E-004	Infinity	1.59626E-005	1.32918E+006
IMA	5.23776E+001	2.12172E+001	-3.00000E+006	-3.58891E+006	1.59626E-005	1.32918E+006

Astigmatism is almost cancelled at the input of the cavity (surface 20) and within the Faraday isolator (surface 6).

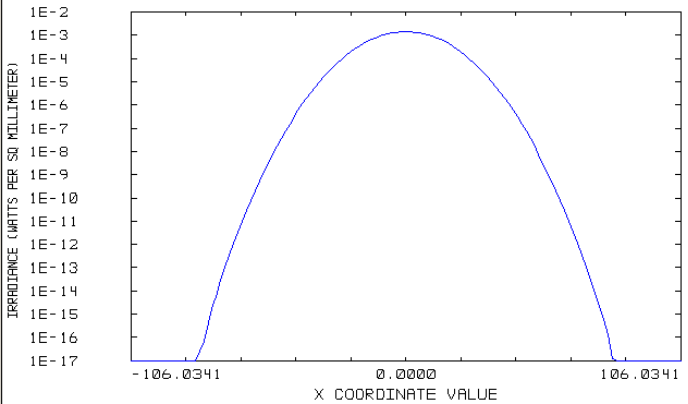


Modeled beam shape @ 17.288m (input mirror location)



TOTAL IRRADIANCE SURFACE 18 #2 WAIST/3 KM ARM

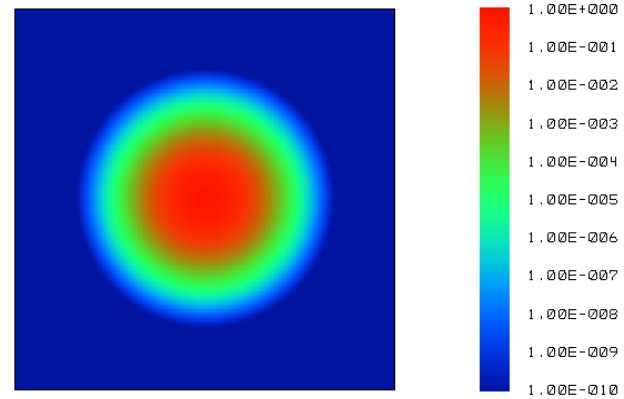
FRI OCT 22 18:16:50 2004
 WAVELENGTH 1.0640 μm AT 0.0000, 0.0000 MM
 DISPLAY X WIDTH = 2.1207E+002, Y HEIGHT = 2.1207E+002 MILLIMETERS
 PEAK IRRADIANCE = 1.4143E-003 WATTS/MILLIMETERS^2, TOTAL POWER = 1.0000E+000 WATTS
 X PILOT: SIZE= 2.1217E+001, WAIST= 2.1217E+001, POS= -1.5864E+000, RAYLEIGH= 1.3291E+006
 Y PILOT: SIZE= 2.1217E+001, WAIST= 2.1217E+001, POS= -1.5877E+000, RAYLEIGH= 1.3291E+006



IRRADIANCE X-CROSS SECTION SURFACE 18 #2 WAIST/3 KM ARM

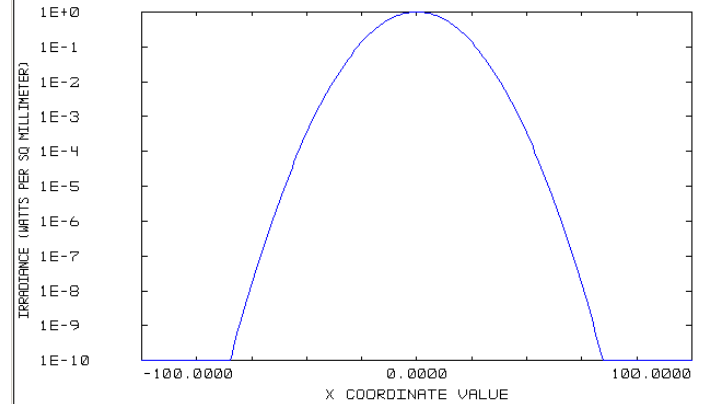
FRI OCT 22 18:21:46 2004
 WAVELENGTH 1.0640 μm AT 0.0000, 0.0000 MM
 CENTER Y = 0.0000E+000
 PEAK IRRADIANCE = 1.4143E-003 WATTS/MILLIMETERS^2, TOTAL POWER = 1.0000E+000 WATTS
 X PILOT: SIZE= 2.1217E+001, WAIST= 2.1217E+001, POS= -1.5864E+000, RAYLEIGH= 1.3291E+006
 Y PILOT: SIZE= 2.1217E+001, WAIST= 2.1217E+001, POS= -1.5877E+000, RAYLEIGH= 1.3291E+006

Ideal (aberration-free) beam shape @ 17.288m (input mirror location)



TOTAL IRRADIANCE SURFACE 18 #2 WAIST/3 KM ARM

FRI OCT 8 2004
 WAVELENGTH 1.0640 μm AT 0.0000, 0.0000 MM
 DISPLAY X WIDTH = 2.0000E+002, Y HEIGHT = 2.0000E+002 MILLIMETERS
 PEAK IRRADIANCE = 1.0000E+000 WATTS/MILLIMETERS^2, TOTAL POWER = 6.2832E+002 WATTS
 X PILOT: SIZE= 2.0000E+001, WAIST= 2.0000E+001, POS= +0.0000E+000, RAYLEIGH= 1.1810E+006
 Y PILOT: SIZE= 2.0000E+001, WAIST= 2.0000E+001, POS= +0.0000E+000, RAYLEIGH= 1.1810E+006

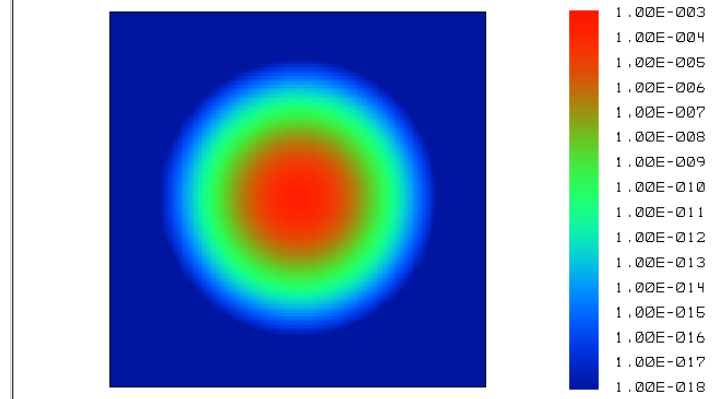


IRRADIANCE X-CROSS SECTION SURFACE 18 #2 WAIST/3 KM ARM

FRI OCT 8 2004
 WAVELENGTH 1.0640 μm AT 0.0000, 0.0000 MM
 CENTER Y = 0.0000E+000
 PEAK IRRADIANCE = 1.0000E+000 WATTS/MILLIMETERS^2, TOTAL POWER = 6.2832E+002 WATTS
 X PILOT: SIZE= 2.0000E+001, WAIST= 2.0000E+001, POS= +0.0000E+000, RAYLEIGH= 1.1810E+006
 Y PILOT: SIZE= 2.0000E+001, WAIST= 2.0000E+001, POS= +0.0000E+000, RAYLEIGH= 1.1810E+006

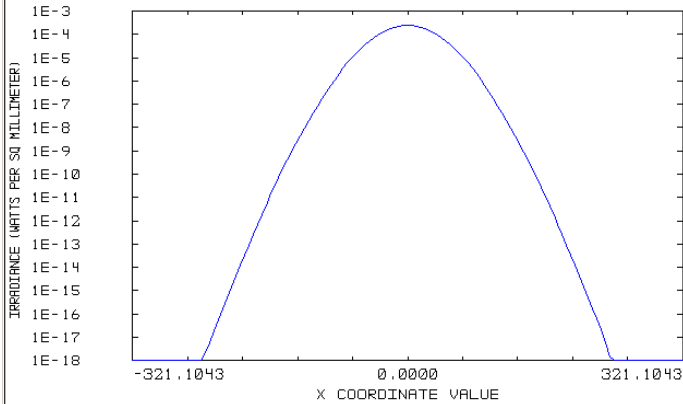
Figure 16: Comparison of the beam size on Fabry-Perot cavities input mirrors at the output of T2 telescope respect to a perfect Gaussian beam.

Modeled beam shape @ 3km



TOTAL IRRADIANCE SURFACE 19 CAVITY END MIRROR

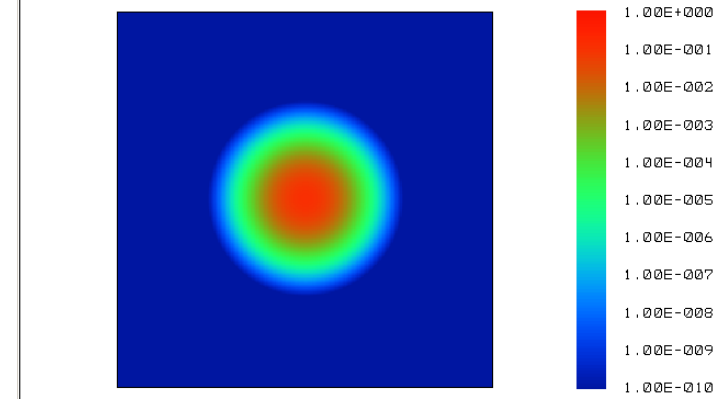
FRI OCT 22 18:21:31 2004
WAVELENGTH 1.0640 μm AT 0.0000, 0.0000 MM
DISPLAY X WIDTH = 6.4221E+002, Y HEIGHT = 6.4221E+002 MILLIMETERS
PEAK IRRADIANCE = 2.4650E-004 WATTS/MILLIMETERS^2, TOTAL POWER = 1.0000E+000 WATTS
X PILOT: SIZE = 5.2378E+001, WAIST = 2.1217E+001, POS = -3.0000E+006, RAYLEIGH = 1.3291E+006
Y PILOT: SIZE = 5.2378E+001, WAIST = 2.1217E+001, POS = -3.0000E+006, RAYLEIGH = 1.3291E+006



IRRADIANCE X-CROSS SECTION SURFACE 19 CAVITY END MIRROR

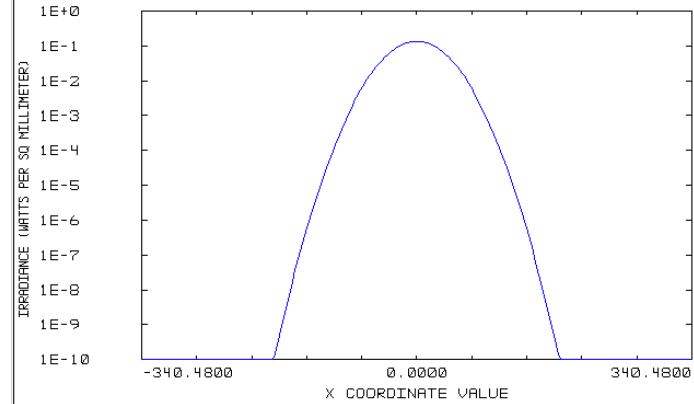
FRI OCT 22 18:21:57 2004
WAVELENGTH 1.0640 μm AT 0.0000, 0.0000 MM
CENTER, Y = 0.0000E+000
PEAK IRRADIANCE = 2.4650E-004 WATTS/MILLIMETERS^2, TOTAL POWER = 1.0000E+000 WATTS
X PILOT: SIZE = 5.2378E+001, WAIST = 2.1217E+001, POS = -3.0000E+006, RAYLEIGH = 1.3291E+006
Y PILOT: SIZE = 5.2378E+001, WAIST = 2.1217E+001, POS = -3.0000E+006, RAYLEIGH = 1.3291E+006

Ideal (aberration-free) beam shape @ 3km



TOTAL IRRADIANCE SURFACE 19 CAVITY END MIRROR

FRI OCT 8 2004
WAVELENGTH 1.0640 μm AT 0.0000, 0.0000 MM
DISPLAY X WIDTH = 6.8096E+002, Y HEIGHT = 6.8096E+002 MILLIMETERS
PEAK IRRADIANCE = 1.3419E-001 WATTS/MILLIMETERS^2, TOTAL POWER = 6.2832E+002 WATTS
X PILOT: SIZE = 5.4597E+001, WAIST = 2.0000E+001, POS = -3.0000E+006, RAYLEIGH = 1.1810E+006
Y PILOT: SIZE = 5.4597E+001, WAIST = 2.0000E+001, POS = -3.0000E+006, RAYLEIGH = 1.1810E+006



IRRADIANCE X-CROSS SECTION SURFACE 19 CAVITY END MIRROR

FRI OCT 8 2004
WAVELENGTH 1.0640 μm AT 0.0000, 0.0000 MM
CENTER, Y = 0.0000E+000
PEAK IRRADIANCE = 1.3419E-001 WATTS/MILLIMETERS^2, TOTAL POWER = 6.2832E+002 WATTS
X PILOT: SIZE = 5.4597E+001, WAIST = 2.0000E+001, POS = -3.0000E+006, RAYLEIGH = 1.1810E+006
Y PILOT: SIZE = 5.4597E+001, WAIST = 2.0000E+001, POS = -3.0000E+006, RAYLEIGH = 1.1810E+006

Figure 17: Comparison of the beam size after 3kms of propagation of the T2 telescope output beam respect to a perfect Gaussian beam.

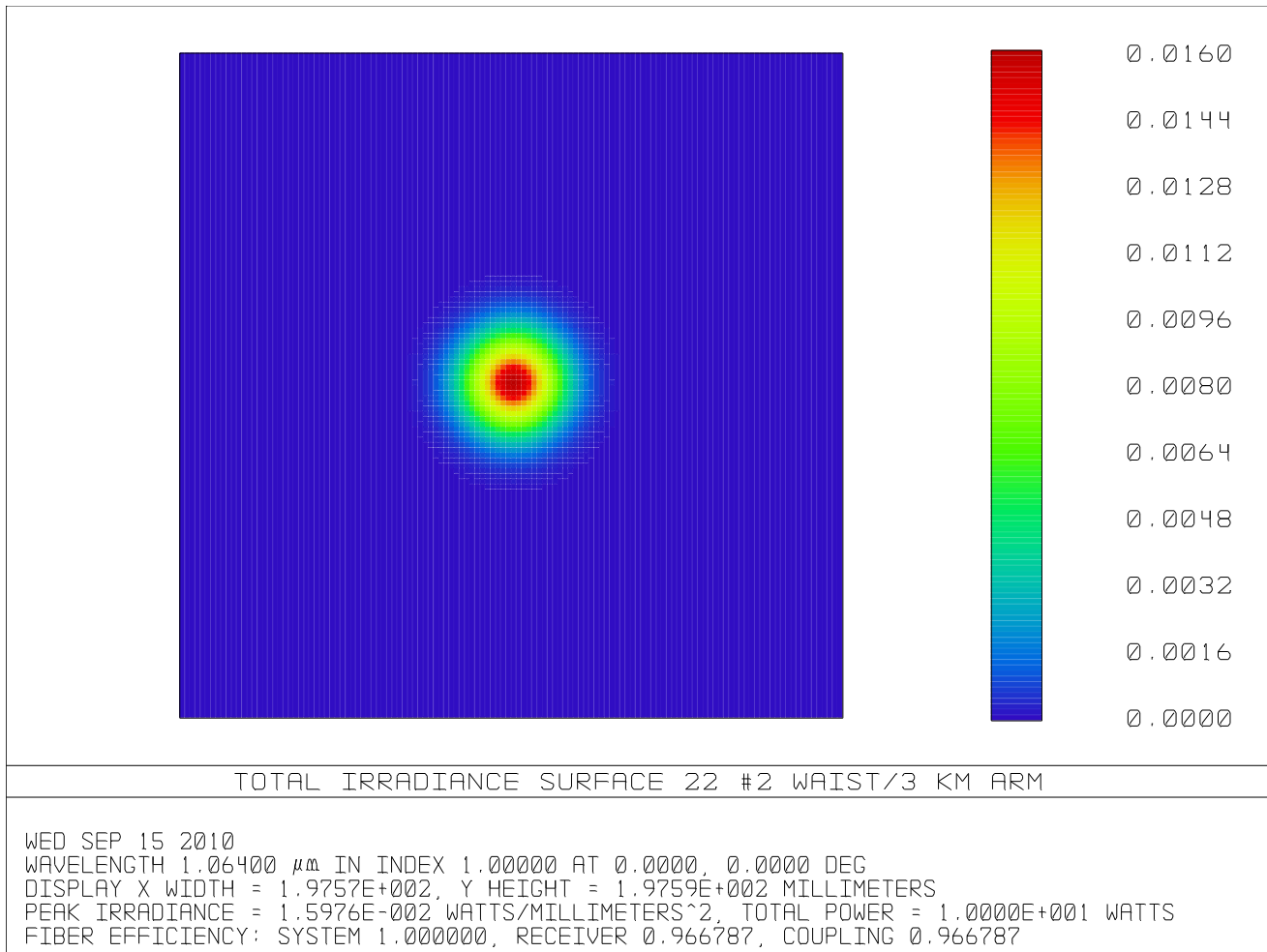


Figure 18: Beam shape at the ITF input and computation of matching on the Fabry-Perot cavities.

On figure 18, as for the spherical mirrors configuration we computed the best coupling expected in the interferometer and we found it to be around 97 % that is definitely much better than with spherical mirrors. If we want to have only a few percent of mismatching on the interferometer the parabolic telescope configuration looks the only solution that we can consider.

3.2.2.3 Influence of M6 (surf. 16) clear aperture on the beam profile @ 3km

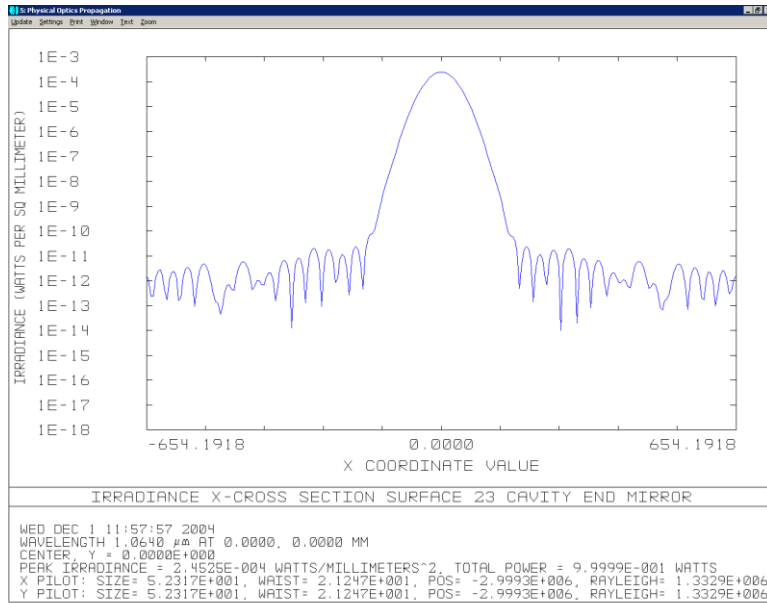


Figure 3-19: Beam profile @ 3km with M6 / 4 inches diameter.

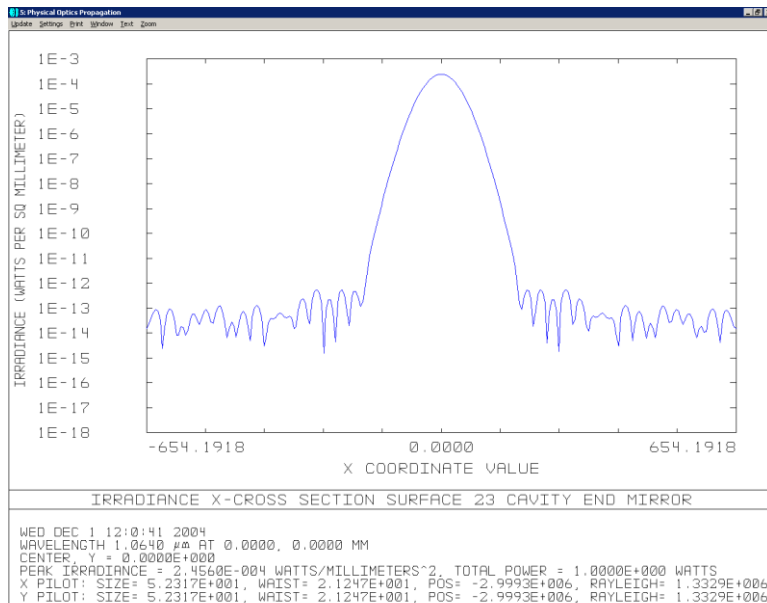


Figure 20: Beam profile @ 3km with M6 / 4.5 inches diameter.

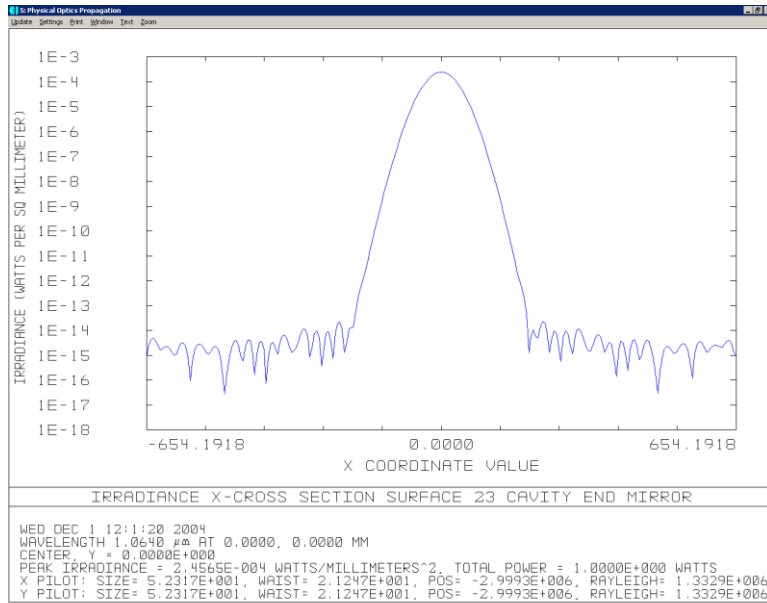


Figure 21: Beam profile @ 3km with M6 / 5 inches diameter.

According to the simulation results showed in figure 19, 20 and 21, we can say that the clear aperture of M6 should be bigger than 4 inches in order to not introduce extra clipping losses.

4. Thermal lensing

The light passing through the Faraday Isolator (back and forth, globally almost 20 W of power) heats the crystal, this inducing a thermal lens effect [1] This thermal lensing changes the focalization of the beam exiting the Input Bench, if it is not compensated by the T1-T2 telescope. For this reason, in order to design and verify the reliability of the T1-T2 telescope, the evaluation of this thermal effect has to be computed.

The FI crystal is modeled by implementing a cylindrical volume (TAFD21/n=1.9326 – 40mm thickness) while the thermal lens effect is modeled by bending the last crystal surface creating thus a positive lens. In order words a spherical lens is introduced in the TGG crystal in order to introduce the thermal lensing effect.

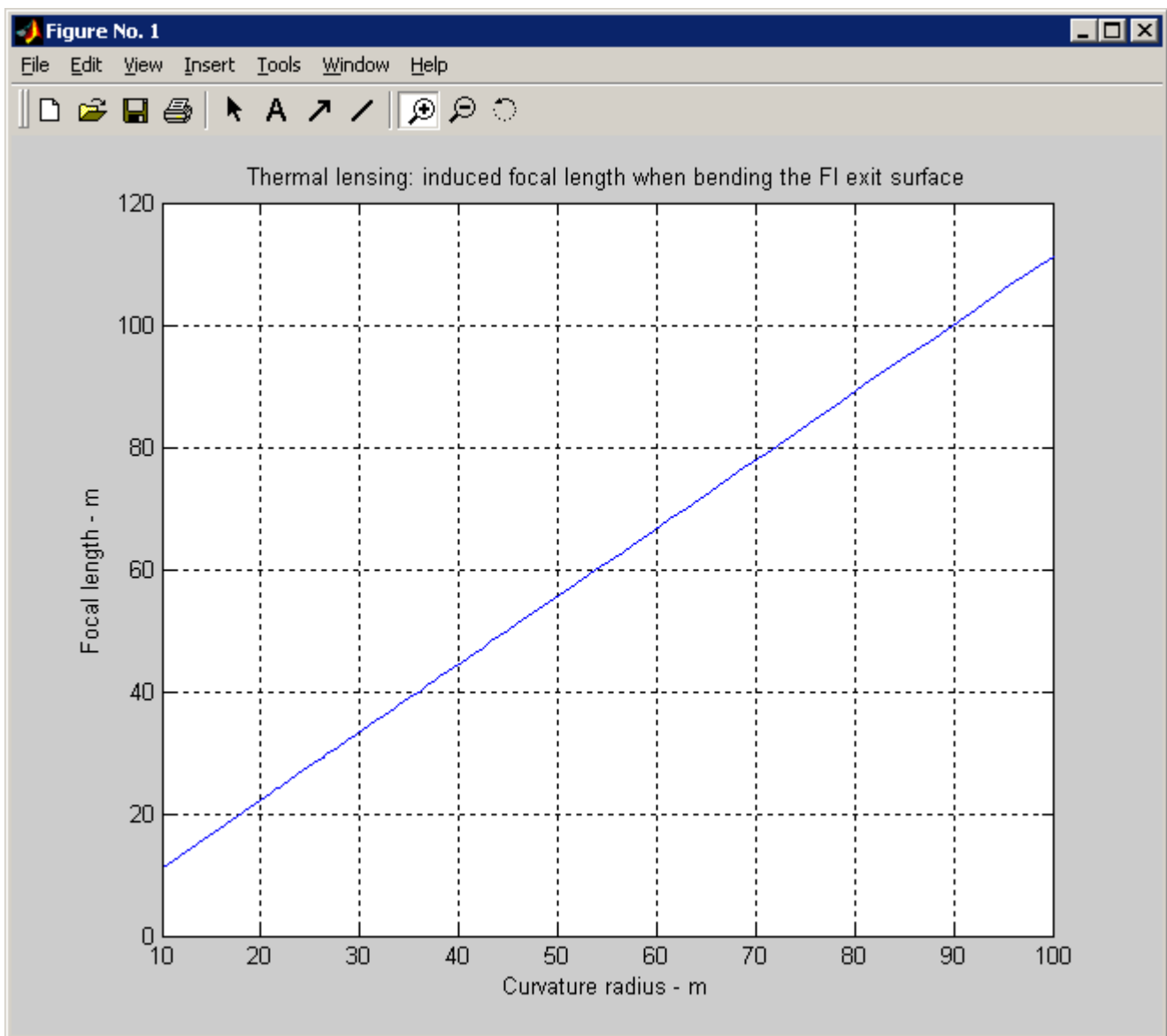



Figure 22: Effective focal lens (EFFL) as the FI last surface curvature is modified

 The logo for VIRGO, featuring a stylized green 'V' composed of three curved lines above the word 'VIRGO' in a bold, sans-serif font.	Note on Virgo Parabolic telescope	Date 09/2010 VIR-0504A-10 Page 32 of 59
--	-----------------------------------	---

On figure 23 and 24, one can see how the waist size and position after the parabolic telescope changes respect to the thermal focal lens introduced in the Faraday isolator magneto-optic crystal (focal length varies between -15m and 15m).

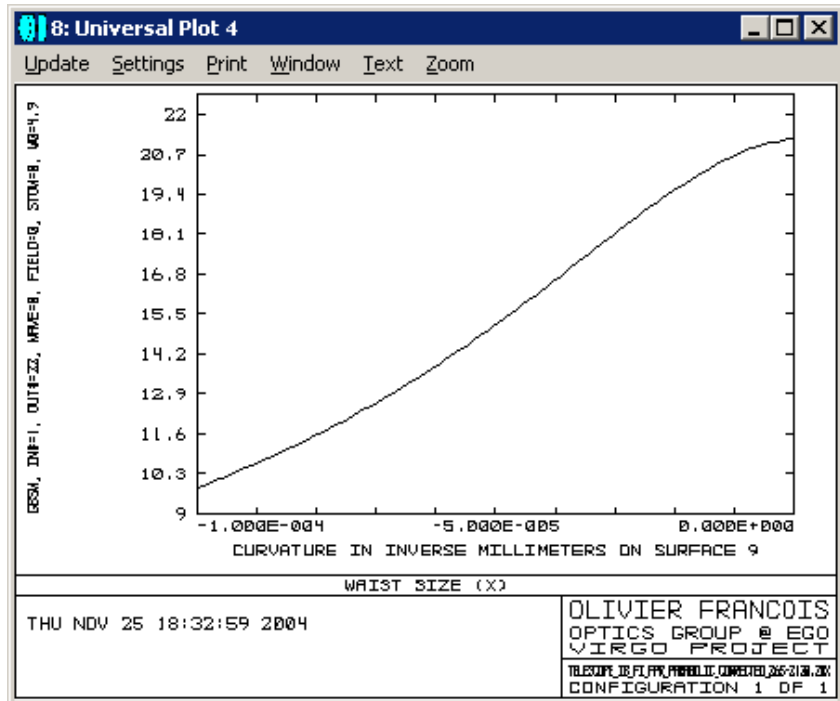


Figure 23: Waist size as the curvature of the FI exit surface is curved from 0.0001mm^{-1} (positive lens with FL/15m) to a plane surface (infinite FL).

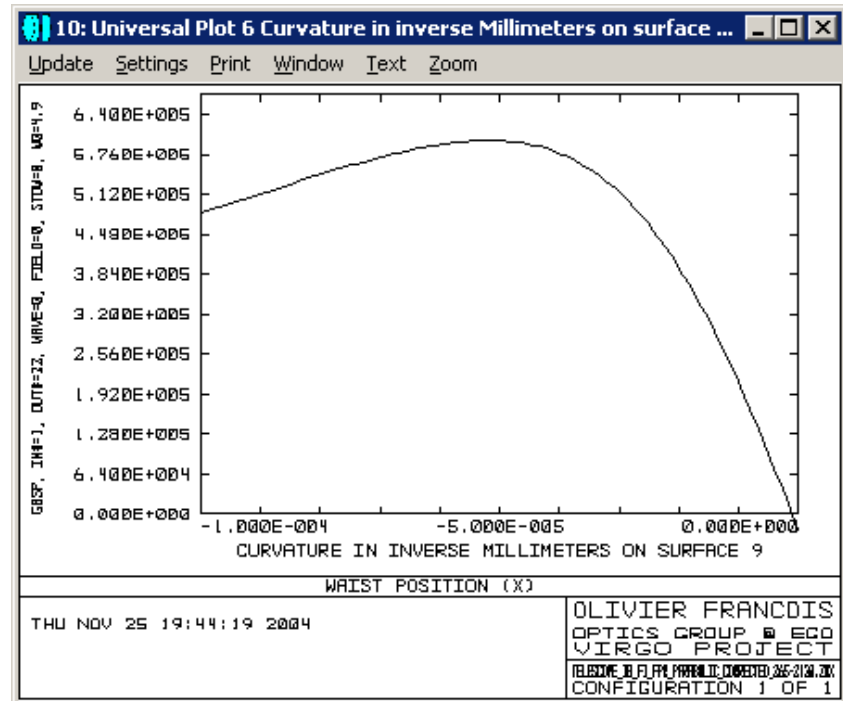


Figure 24: Waist position as the curvature of the FI exit surface is curved from 0.0001mm^{-1} (positive lens with FL/15m) to a plane surface (infinite FL).

In order to circumscribe the thermal lens effect we study here the possibilities to compensate the MF worsening by adjusting T1 or T2 separation.

4.1. Thermal lensing compensation by adjusting T1 separation

Setting the equivalent thermal focal lens to a low value **11m** which produces a severe impact on the optical performances and is the worth case expected for Virgo and Virgo+ according to the maximum laser power sent into the Faraday, we estimate hereafter how modifying the separation distance between the two lenses forming the T1 telescope can help us to recover decent performances.

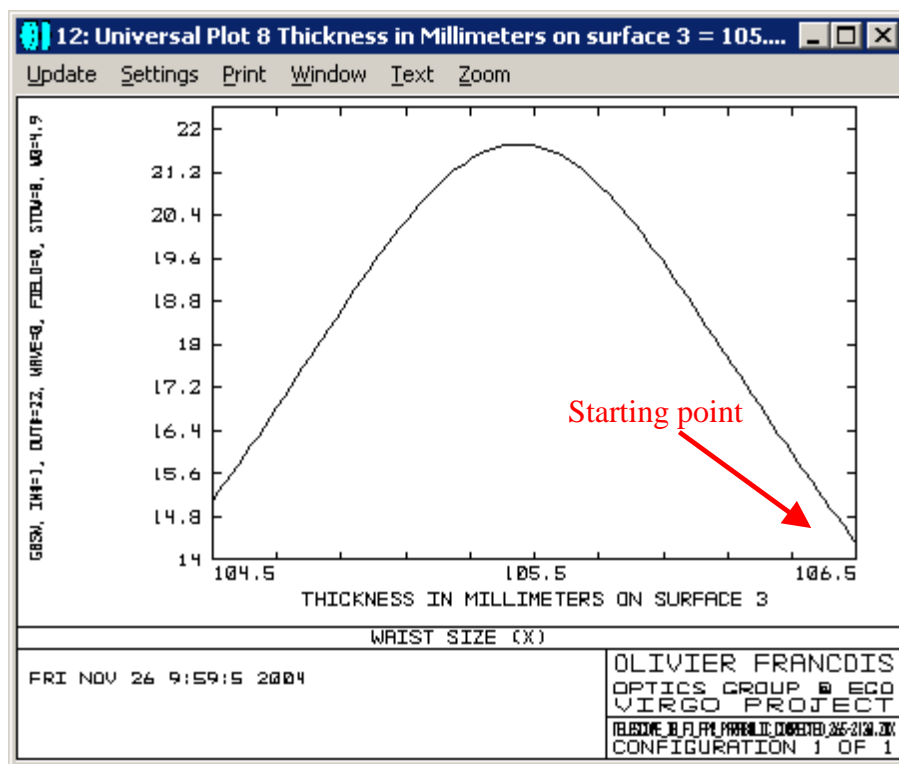


Figure 25: Waist size as the thermal lensing effect occurs and the T1 separation is modified.

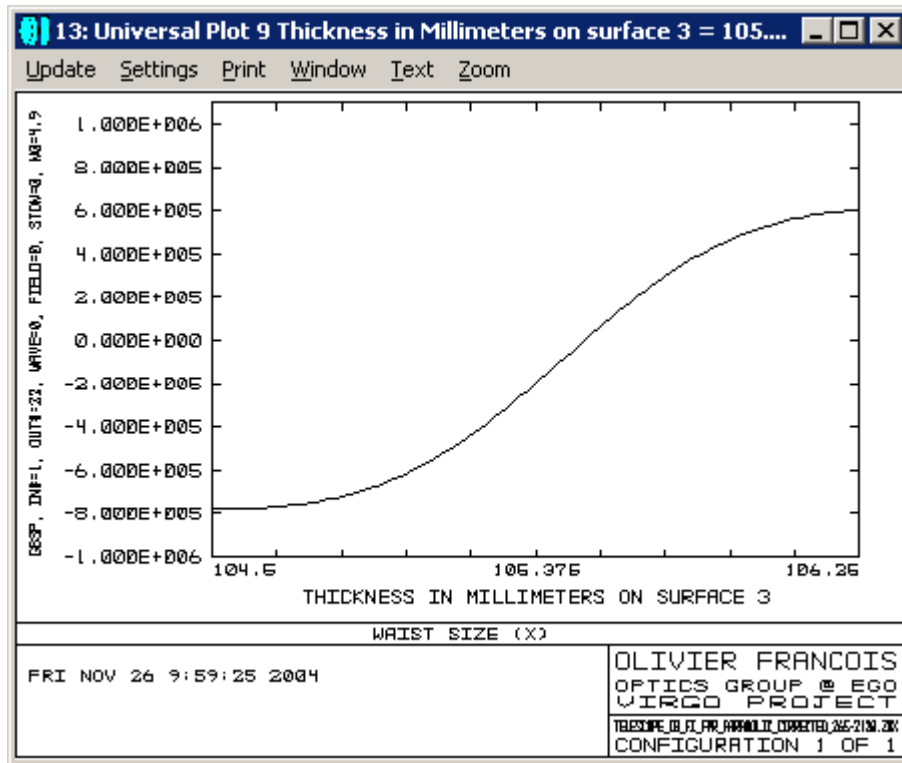


Figure 26: Waist position as the thermal lensing effect occurs and the T1 separation is modified.



We have simulated the thermal lens effect by incurving the TGG crystal output surface (radius of curvature=10m (see figure 27) corresponding to a Faraday focal length of about 11m).

Surf: Type	Comment	Radius	Thickness	Class	Semi-Diameter
OBJ	Standard	Infinity	Infinity		0.000000
1	Standard	INPUT WAIST	200.000000		0.000000 U
2*	Standard	T1-LENS#1	129.428679	BK7	12.700000 U
3*	Standard	T1-LENS#2	Infinity		12.700000 U
4*	Standard	T2-LENS#2	Infinity	BK7	12.700000 U
5*	Standard	T2-LENS#2	70.000000		12.700000 U
6*	Standard	ENT APERT FI	Infinity		10.000000 U
7*	Standard		20.000000	TAFD21	10.000000 U
8*	Standard	WAIST #1-FI CENTER	Infinity	TAFD21	10.000000 U
9*	Standard		-1.000000E+004		10.000000 U
10*	Standard	EXIT APERT FI	Infinity		10.000000 U
11	Coordinate B..		0.000000	-	0.000000
12*	Standard		0.000000	MIRROR	25.400000 U
13	Coordinate B..		-550.000000	-	0.000000
14	Coordinate B..		0.000000	-	0.000000
ST0*	Standard	T2-PAR MIRROR #1	150.000000	MIRROR	25.400000 U
16	Coordinate B..		675.059331	-	0.000000
17	Coordinate B..		0.000000	-	0.000000
18*	Standard	T2-PAR MIRROR #2	-1200.000000	MIRROR	50.000000 U
19	Coordinate B..		-5288.000000	-	0.000000
20*	Standard	FLAT POWER RECYCL..	Infinity	SUPRASIL	80.000000 U
21*	Standard	CAVITY INPUT	Infinity		100.000000 U
22	Standard	#2 WAIST/3 KM ARM	Infinity		0.000000 U
IMA	Standard	CAVITY END MIRROR	Infinity		0.000000 U

Figure 27: Faraday isolator with equivalent thermal lens (11m focal length)

Without modifying the telescope settings, the waist size becomes 9.9 mm (instead of 21.2 mm) located 481 m before the cavity input.

By adjusting the separation distance of the first telescope (see figure 27 – T1 lens#2 // T2 lens#1), it is possible to compensate for the waist worsening (and even to over-compensate the waist decrease).

Waist characteristics	X-Waist	Y-Waist	X-Position	Y-Position
Before compensation (Separation=107.262mm)	9.83mm	9.83mm	481m	481m
After compensation (Separation=105.34mm)	21.86mm	21.86mm	-3.51m	+3.51m
Ideal values	21.2mm	21.2mm	0	0
Optimum Design values (without lensing effect)	21.214mm	21.214mm	3.7E-4* (* M5/6 tilts)	4.5e-4* (* M5/6 tilts)

Table 1 - Thermal lensing compensation by acting on T1 separation

4.2. Thermal lensing compensation by adjusting T2 separation

Setting the equivalent thermal focal lens to an arbitrary low value **11 m**, which produces a severe impact on the optical performances, we estimate hereafter how modifying the separation distance between the two mirrors forming the T2 telescope can help us to recover decent performances.

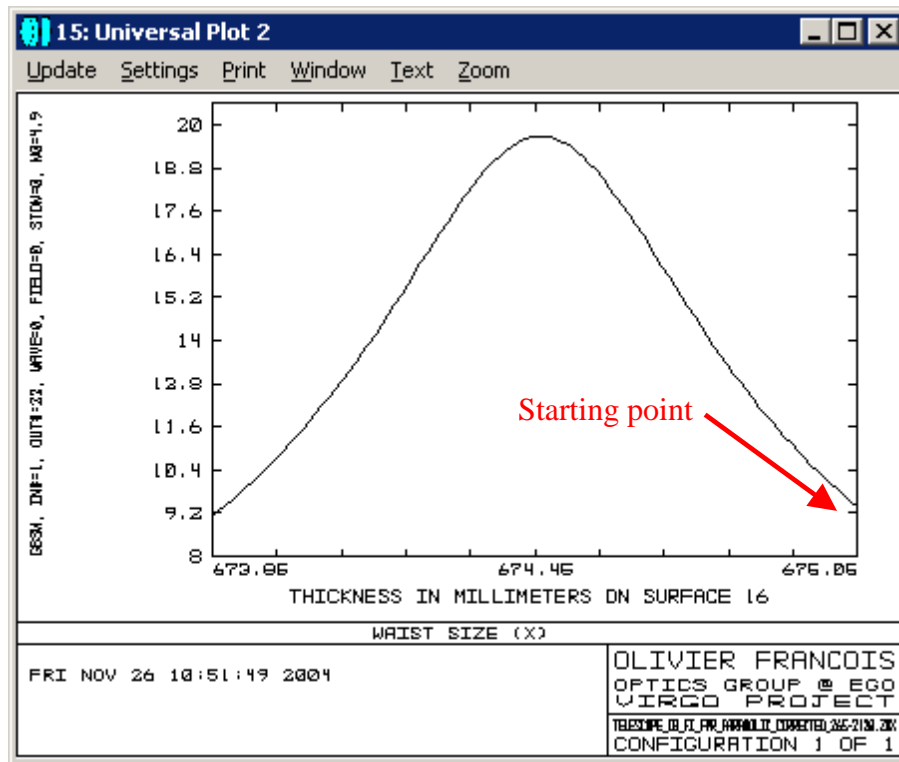


Figure 28: Waist size as the thermal lensing effect occurs and the T2 separation is modified.

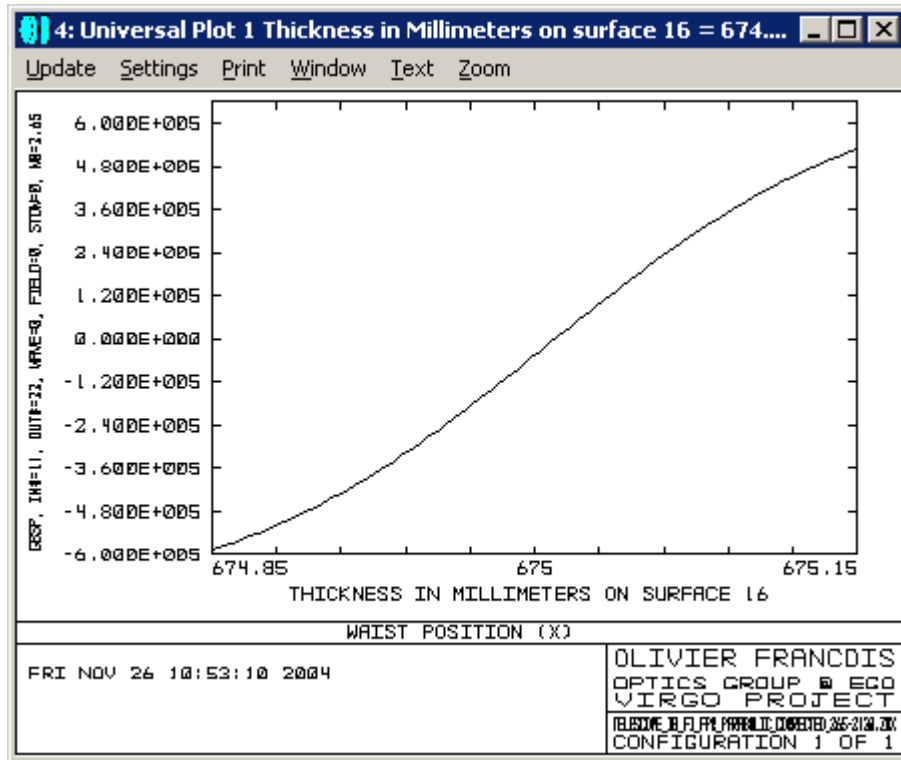


Figure 29: Waist position as the thermal lensing effect occurs and the T2 separation is modified.

By adjusting the separation distance of the second telescope, it is possible to partially compensate for the waist worsening. One has to note that in this case it is not possible to retrieve a waist size over 20mm.

Waist characteristics	X-Waist	Y-Waist	X-Position	Y-Position
Before compensation (Separation=675.014mm)	9.83mm	9.83mm	478m	478m
After compensation (Separation=674.457mm)	19.684mm	19.669mm	-27.9m	+28.8m
<i>Ideal values</i>	<i>21.2mm</i>	<i>21.2mm</i>	<i>0</i>	<i>0</i>
<i>Optimum Design values (without lensing effect)</i>	<i>21.214mm</i>	<i>21.214mm</i>	<i>3.7E-4*</i> <i>(* M5/6 tilts)</i>	<i>4.5e-4*</i> <i>(* M5/6 tilts)</i>

Table 2 - Thermal lensing compensation by acting on the distance between M5 and M6 (mirrors of T2 telescope).

5. Compensation of MC curvature errors

As a last check, the impact on the telescope performances of MC mirror curvature errors is evaluated. The expected error on the waist size at the MC output has been evaluated to be in the range $\pm 0.2\text{mm}$ corresponding to an error on IMC end mirror radius of curvature (ROC) of about $\pm 7\text{m}$ as you can see on figure 30. Thus we propose to assess in the following chapter how to compensate thanks to T1 and/or T2 a waist varying in the range 4.7-5.1mm.

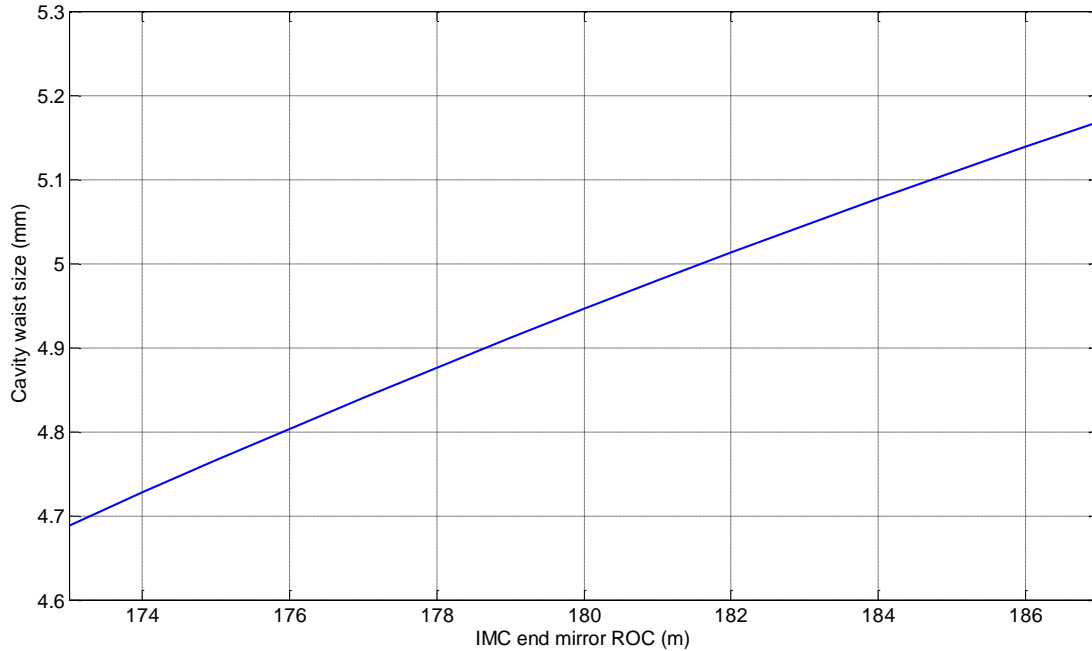


Figure 30: IMC cavity waist size function of IMC curved mirror radius of curvature..

5.1. Compensation with T1 separation

The following results were obtained using T1 lenses made with “Special Virgo fused silica”

Waist size range	Lower limit <i>-4.7mm-</i>	Nominal value – Optimal design <i>-4.9mm- Fused silica SV</i>	Higher limit <i>-5.1mm-</i>
Waist size-X	20.33	21.20	22.07
Waist size-Y	20.33	21.20	22.07
Waist position-X	-11.16	-2.26	8.19
Waist position-Y	-7.35	-2.22	13.46
T1 separation	124.472	124.459	124.447
<i>T2 separation*</i>	<i>675.014</i>	<i>675.014</i>	<i>675.014</i>

**fixed value*

Adjusting T1 separation does not allow us to retrieve the ideal waist size. For both cases –smaller and larger input waist- the size mismatch can only be reduced to about 4.1%.

5.2. Compensation with T2 separation

The following results were obtained using T1 lenses made with “Special Virgo fused silica”

Waist size range	Lower limit <i>-4.7mm-</i>	Nominal value – Optimal design <i>-4.9mm- Fused silica SV</i>	Higher limit <i>-5.1mm-</i>
Waist size-X	20.34	21.20	22.06
Waist size-Y	20.34	21.20	22.06
Waist position-X	-184	-2.26	216
Waist position-Y	176	-2.22	-209
<i>T1 separation*</i>	<i>124.459</i>	<i>124.459</i>	<i>124.459</i>
T2 separation	675.017	675.014	675.011

**fixed value*

Adjusting T2 separation does not allow us to retrieve the ideal waist size. For both cases –smaller and larger input waist- the size mismatch can only be reduced to about 4.06%.

5.3. Compensation with T1 and T2 separations

The following results were obtained using T1 lenses made with “Special Virgo fused silica”

Waist size range	Lower limit <i>-4.7mm-</i>	Nominal value – Optimal design <i>-4.9mm- Fused silica SV</i>	Higher limit <i>-5.1mm-</i>
Waist size-X	20.34	21.20	22.07
Waist size-Y	20.34	21.20	22.07
Waist position-X	-121	-2.26	82
Waist position-Y	117	-2.22	-80
T1 separation	124.463	124.459	124.452
T2 separation	675.016	675.014	675.013

Adjusting simultaneously T1 and T2 separations does not allow us to retrieve the ideal waist size. For smaller input waist –4.7mm- the size mismatch can only be reduced to about 4.06% and for larger input waist –5.1mm- the size mismatch can be reduced to about 4.1%.

5.4. Compensating by replacing the T1 first lens

Waist size range	Lower limit <i>-4.7mm-</i>	Nominal value – Optimal design <i>-4.9mm- Fused silica NON-SV</i>	Higher limit <i>-5.1mm-</i>
Waist size-X	21.24	21.20	21.24
Waist size-Y	21.24	21.20	21.24
Waist position-X	-6.68	2.72	-6.12
Waist position-Y	6.93	-1.76	6.41
T1-lens#1 Curvature radius	124	129.5	134.5
T1 separation	109.661	121.883	132.993
T2 separation	675.016	675.014	675.014

Adjusting the curvature radius of the entrance lens (T1) and modifying the separation distance of mainly T1 and alternatively T2 allows us to better tune the waist size/position. The differences with respect to the ideal values are at the end below 2/1000 for the sizes and do not exceed 7mm for the positions.

6. Parabolic telescope (T2) pre-alignment

The pre-alignment of the input telescope -performed out of the vacuum tower- consists in setting-up the best -in air- level of confocality. Once in the vacuum the only main adjustment to be performed should be the focus (e.g. longitudinal separation). This means that the main adjustments in term of tilts, lateral and vertical correction shall be performed during this step.

Two procedures have been tested successfully during the visit at CalTech (19th, January - 29th, January). Here follows a presentation of these procedures.

6.1. Single pass method with two autocollimators

The procedure described hereafter has already been applied successfully at Ligo.

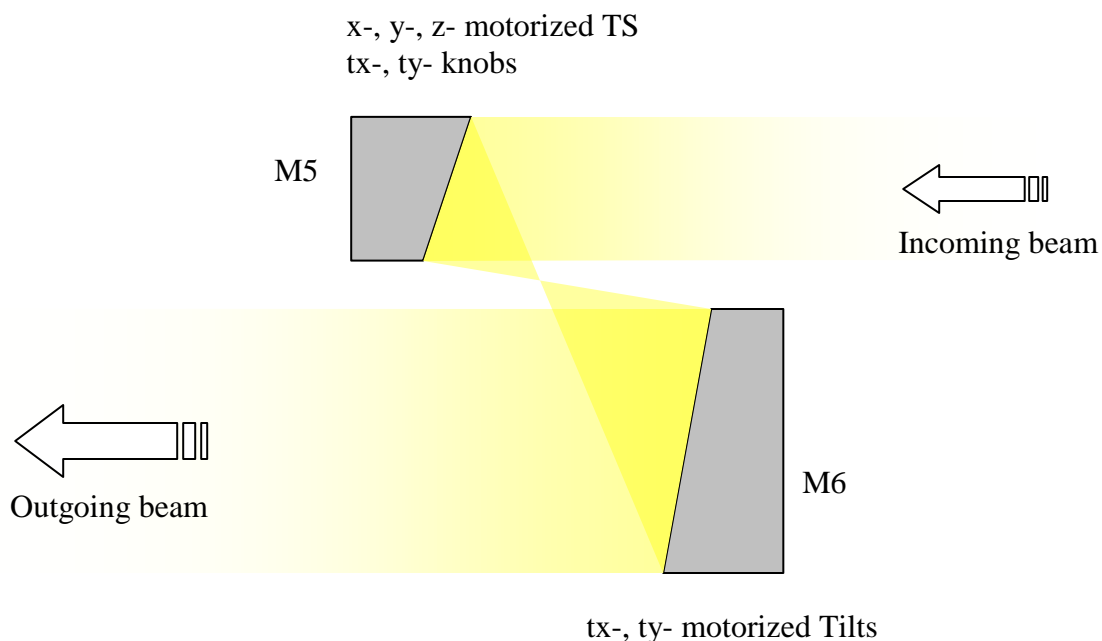


Figure 31: Scheme of the off-axis parabolic telescope and its degree of freedom

A first rough adjustment must be performed consisting in aligning the autocollimators direction onto the mirror axis, positioning the mirrors very close to their working conditions in term of longitudinal separation (sum of the focal lengths with reference at the mirror centers) and lateral separation (sum of the off-axis distances with reference at the mirror centers). The procedure makes use of three reference flats: all these flats have faces perfectly parallel (within a few arcsecs); the first flat, used for the autocollimator alignment (AC-Flat), needs both faces polished. One (M5-Flat) flat is fit for the M5 mount, and only one reflective face is needed. The third flat (M6-Flat) is fit for M6 mount, and also there only one reflective face is needed. All mirror mounts should be kinematik, with three supporting points for the mirror back surface. All mounts should be blockable.

Step #1 – M5 alignment on reference flat

- Check the centering of the beam on M5 mirror.
- The autocollimator #1 being focused at infinite, remove the M5 mirror and align the autocollimator on the AC-FLAT. The AC-Flat position should be setup with respect to external references (north arm references, mode cleaner mirror ...).
- Insert M5-Flat mirror within the M5 holder then align back surface plane of the mount on the autocollimator direction previously determined.
- Block the M5 mount. Replace the M5-Flat mirror with M5 parabolic mirror.
- Check the centering of the beam on M5 mirror. If necessary shift the autocollimator and restart Step #1 from scratch.

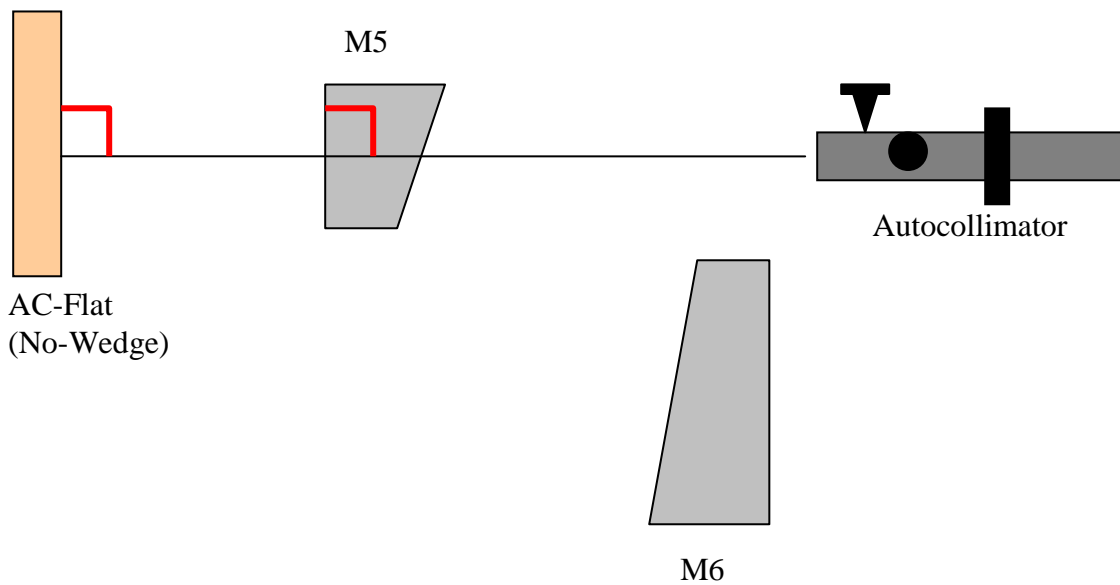


Figure 32: Step #1: M5 alignment on reference flat

Step #2 – M6 alignment on the reference flat

- Place the AC-Flat in front of M6 mirror without losing the initial direction. This can be performed by using either a shift method or by placing the reference flat along a mechanical guide.
- Once the AC-Flat is facing M6, align the second autocollimator (focused at infinite) with respect to the given direction.
- Exchange the M6 parabolic mirror with the M6-Flat mirror.
- Remove the AC-Flat (if necessary) then align M6-Flat mirror (i.e. M6 mount) along the direction previously determined.
- Block the M6 mount. Take out the M6-Flat mirror of the mount and replace it with M6.

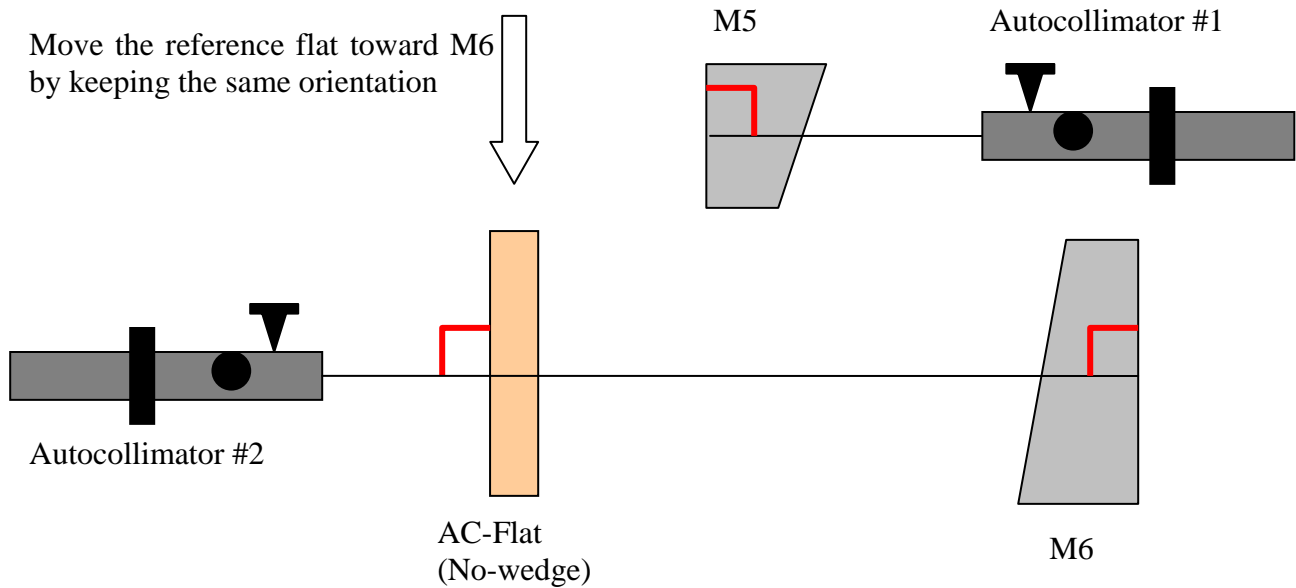
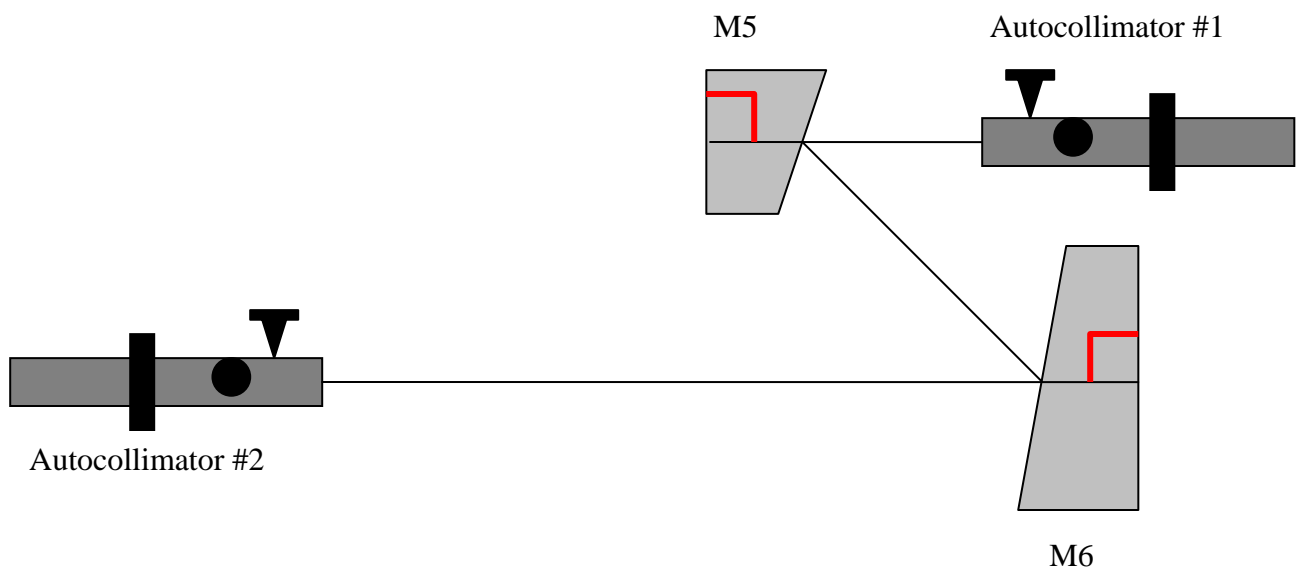


Figure 33: Step #2: M6 alignment on the reference flat

Because of the requirements on the perpendicularity of the mirrors back-surface the mother parabola axis of both mirrors is now aligned with the direction given by the reference flat ($\pm 0.03^\circ$).

Step #3 – The single pass method

- Unblock all mirror mounts.
- Check the centering of the beam on M6 mirror. An adjustment can be performed by acting either on M5 clock orientation within its mount (probably not the better solution) or by moving up/down the M6 mirror.
- The autocollimator #1 is now used only as a projector. The autocollimator #2 is used to monitor the incoming beam.
- The aim is to retrieve the projected reticule pattern (emitted by the autocollimator #1) by adjusting the longitudinal separation. In case of lateral displacement (check the beam position on the autocollimator #2 entry surface), try to compensate by adjusting the lateral separation.
- The off-axis parabolic telescope is setup to infinity (e.g. in an afocal configuration) when the projected pattern is clearly visible through the autocollimator #2. Try to optimize the pattern visibility mainly by acting on the translation degree of freedom.



6.2. Figure 34: Step 3: The single pass method Double pass method with a single autocollimator and a couple laser/beam expander.

The procedure describe hereafter has been applied successfully on a 1x breadboard telescope during the EGO mission at CalTech (19th - 29th January 2005). This is an alternative to the previous method in case where only one autocollimator is available but it requires the use of a laser together with a beam expander.

Step #0 – Rough adjustment

A first rough adjustment must be operated consisting in positioning the mirrors very close to their working conditions in term of longitudinal separation (sum of the focal lengths with reference at the mirror centers) and lateral separation (sum of the off-axis distances with reference at the mirror centers).

Step #1 – Alignment of M5 & M6 mirrors with respect to the AC-Flat.

The procedure to be applied here is identical to the alignment described previously in chapter 6 / Steps 1&2.

Step #2 – Alignment of the laser

- Replace the M5 mirror with the M5-Flat.
- Check that the beam expander focus is set to infinity.
- Align the combination laser/beam expander with respect to the flat mirror by verifying the position of the reflected beam that should passed through the pinhole/iris center hole. Moreover the incoming laser beam has to be centered on the M5-Flat (i.e. the M5 mirror when replaced).

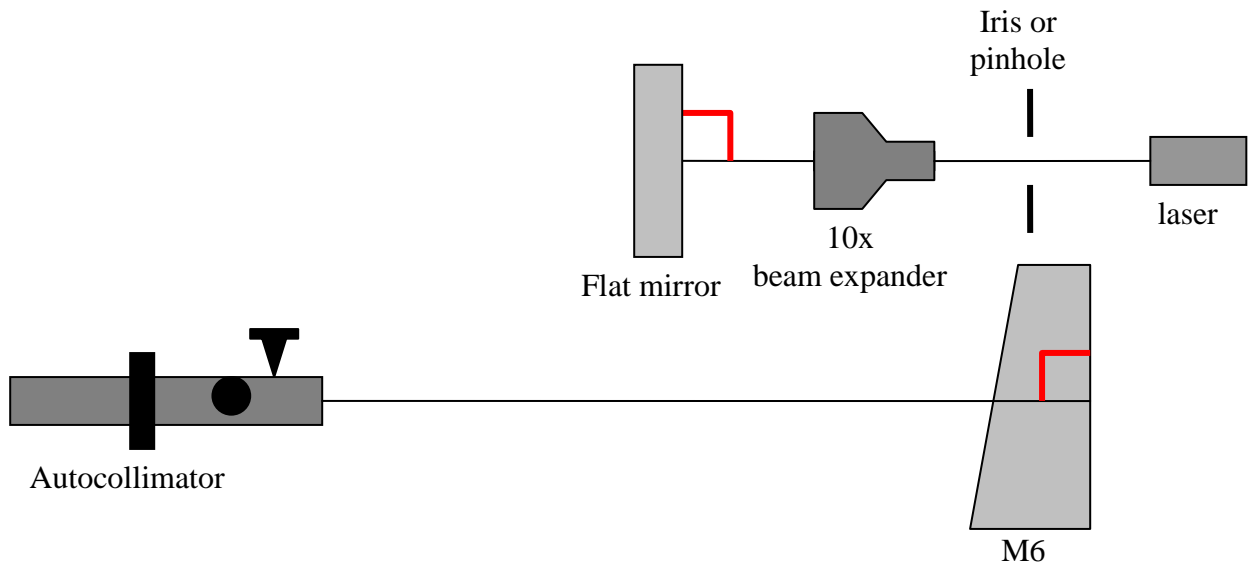


Figure 35: Step #2.

Step #3 – Reaching the vicinity of the afocal condition

- Block the M5 mount. Unmount the M5-Flat mirror and place the M5 mirror within its mount.
- Check the centering on M6 mirror and verify the position of the beam on the autocollimator aperture. If necessary perform an adjustment by tuning the lateral separation, the vertical position of M6 mirror and the clock orientation.
- The afocal condition can be reached by adjusting the longitudinal separation and eventually the lateral distance (the smaller the spot size on the autocollimator output monitor, the better the afocal condition).

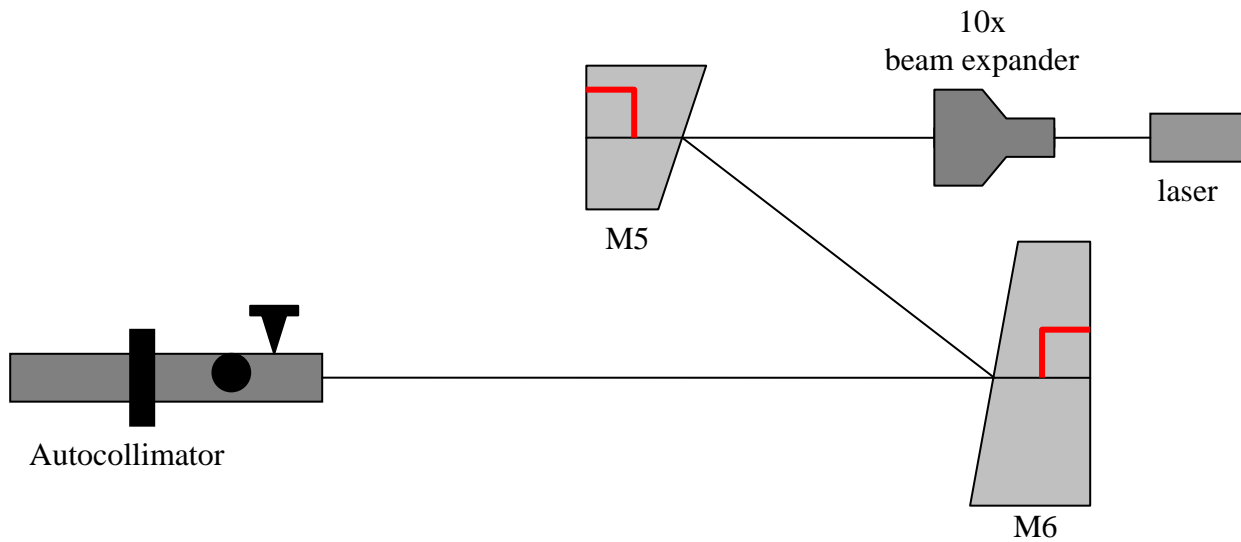


Figure 36: Step #3.

Step #4 – Fine tuning of the afocal condition: double pass method

- Place a flat mirror at the M5 output side of the telescope and align the mirror in order to get back the reflected light into the autocollimator.
- Fine tune the focus (longitudinal separation) and eventually the lateral separation (off-axis distance) in order to optimize the image quality of the reticule pattern.

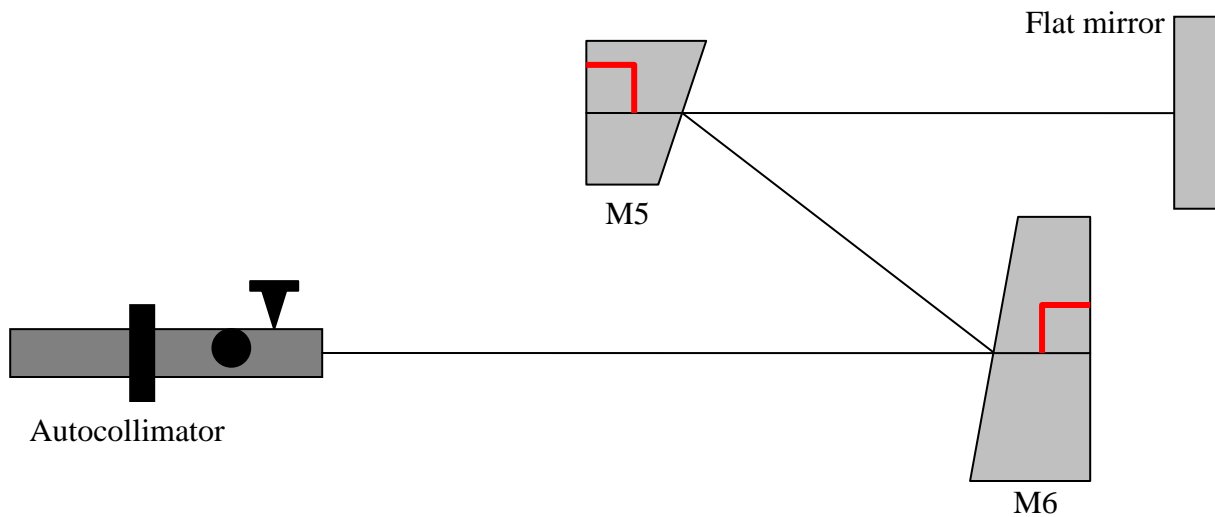


Figure 37: Step #4.

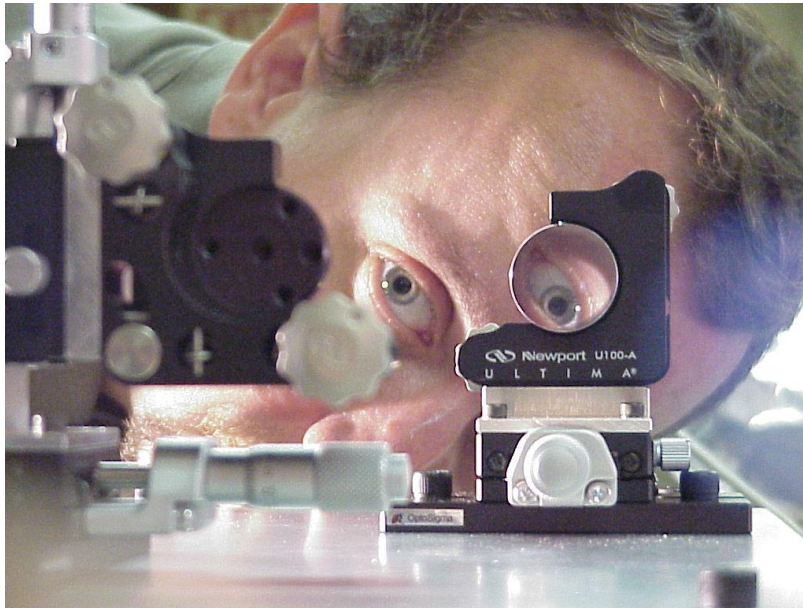


Figure 38: Example of the final configuration of a pretty well aligned off-axis parabolic telescope.

7. Commissioning of the parabolic telescope.

7.1. Overview of the commissioning

As already explained previously, it has been decided to use a reflective off-axis parabolic telescope since the design showed that, when properly aligned, this telescope would have been almost aberration free. At the moment of the Injection Bench design the level of aberration was fixed in order not to have a mismatching with the interferometer bigger than 4 % (at least 96% matching). The installed off-axis parabolic telescope has matched this requirement.

When properly aligned and centered the mismatching is less than 2% (1.5% has been reached see logentry [#13829](#)). The mismatching was of the order of 3% (see logentry [#12127](#)) with 8 W laser power transmitted by the IMC cavity and the PR mirror misaligned by 150 urad (this means that about 16 W of laser power are passing through the Faraday isolator).

The mode matching could be improved and we were able to reach a matching higher than 98% with this input power.

With 17 W laser power, we measured a mismatching of about 3% that increases to about 9% when the PR mirror is aligned (meaning that we have about 34 W laser power in the Faraday isolator)(see logentry [#23018](#)). As far as we know there is no noise introduced by the residual mismatching of the beam on the interferometer. That is why we did not optimized the matching on the Interferometer at the time we installed the new SIB but as explained in section 4 by tuning properly T1 and T2 telescopes we could be able to recover the mismatching on Virgo.

The matching optimization has been done in June 2010 in order to reduce the asymmetry of the matching on the 2 Fabry-Perot cavities after the installation of the new Virgo+ mirrors in Spring 2010 (see section 7.3 for further details).

Nevertheless, some problems were encountered during the commissioning of this telescope:

1) The two M5 and M6 mirrors of the telescope were carefully aligned one with respect to the other in clean room on the bench following the procedure explained in section 6. It was impossible to guarantee the global telescope pointing with respect to the bench axis better than an estimated value of 1 mrad. It was planned that the likely residual pointing alignment of the telescope had to be performed by turning the bench. We had to rotate the bench by about 800 μ rad (see logentries [#12036](#) and [12039](#)). The operation was somehow slow because it was necessary to move at the same time the Beam Monitoring System (BMS) control to keep the IMC aligned and locked and the steering mirrors of the RFC to keep it aligned (see logentries [#12054](#), [12064](#), [12070](#), [12080](#), [12084](#)).

NB: In order to optimize in an easier way the telescope performance it would have been better to align the parabolic telescope separately from the RFC alignment which is not completely the case for the current SIB mainly due to space constraints. In future upgrades of the SIB, we should find a way to decouple more the alignment of the parabolic telescope from the RFC cavity alignment. A possible improvement consists of making larger and remotely tunable the two mirrors of the periscope (SIB_M11 and SIB_M12) or to pick the beam for the reference cavity right after the IMC cavity (before the FI in order to avoid that the matching on the RFC changes with the laser power travelling through the FI).

2) The tuning of the parabolic telescope has been long: this comes out from the above mentioned coupling but also from needs lately become more stringent than what was required at the beginning:

- the telescope was meant to provide a matching of about 96%, it was asked later to improve it, which has been actually possible. It has to be noticed that, with the previous telescope, a spherical mirror telescope, the intrinsic astigmatism yielded already, in the optimal centered and aligned condition, more than 3.5% astigmatism. And no attempt to optimize this telescope has never been done, the mismatching having been larger than 4% up to C7 commissioning run.

Furthermore, before recently, no attempt at all to center the suspended mirrors had been tried: this together to the impossibility to move (for example to raise) beyond a certain level the suspended Injection Bench, imposes further constraints to the alignment of the injection telescope. All these problems have come out after the new SIB installation, and the bench has met these new requirements, even if requiring some commissioning time. Either with the previous spherical telescope, and very likely with a refractive one the same problems would have occurred. In future design of telescopes these new problems should be better taken into account.

7.2. Use of Zemax software during the telescope optimization process: Example 1.

Zemax software has been extensively used during the design phase of the new SIB and especially for the parabolic telescope. Moreover, we used it a lot to optimize the parabolic telescope tuning as it is explained in the following paragraph.

For example, we could see after the IMC cavity relock and the ITF realignment (at the beginning of 2006) that the ITF reflected beam had a strange shape as shown in figure 39.

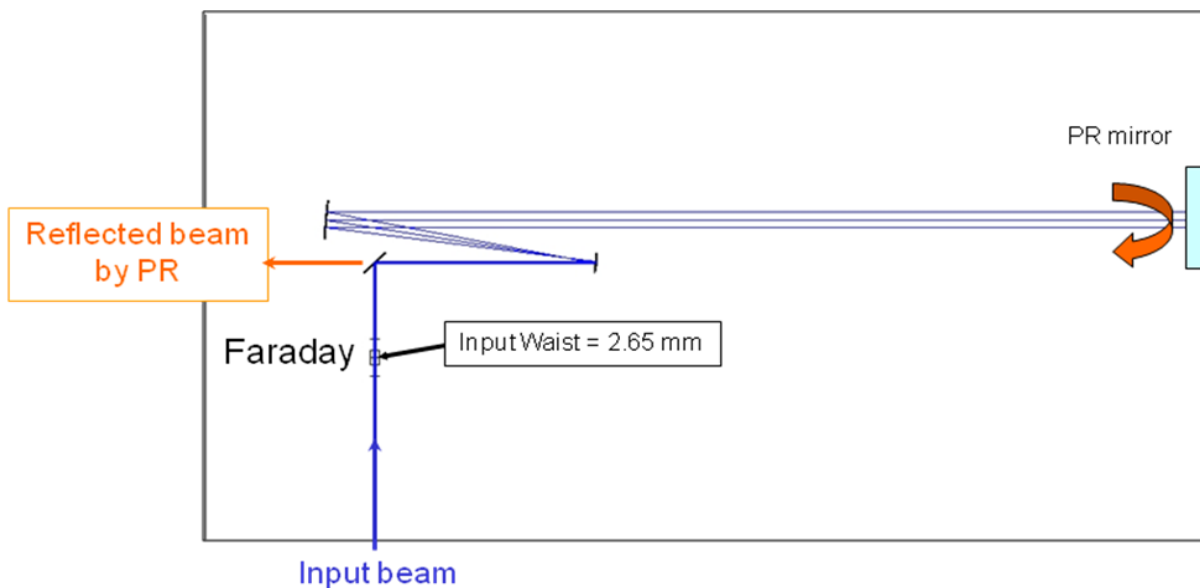


Figure 39: Experimental setup.

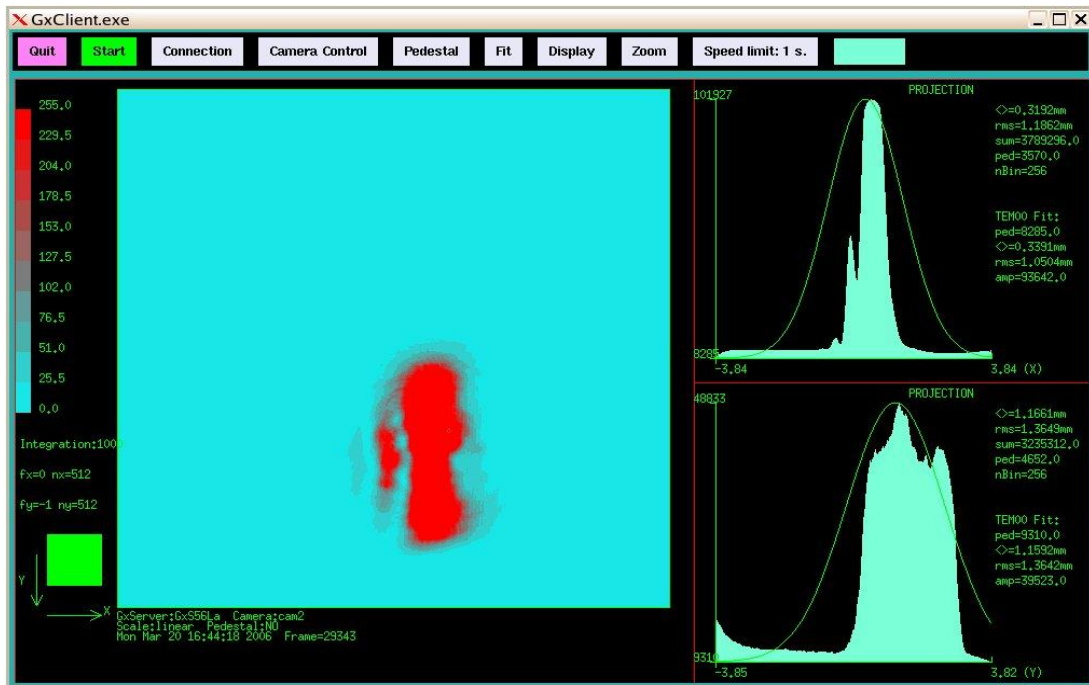


Figure 40: View of the beam as seen on Camera 2 (ITF reflection) on the External Injection Bench in March 2006.

In order to understand the strange shape, we did a simulation with Zemax. Hereafter is given the configuration used for the simulation (see figure 41).

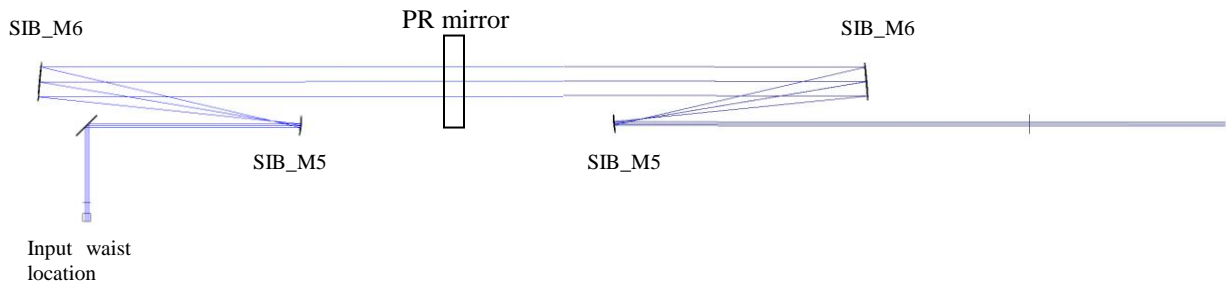


Figure 41: Zemax optical setup used for the simulation.

The configuration presented in figure 41 has been done so that we can still use the sequential mode of Zemax that enables to use the physical optical propagation feature. The input waist considered is: $w_x=2.65\text{mm}$; $w_y=2.65\text{mm}$ located 83 cm before SIB_M5 (the first mirror of the parabolic telescope).

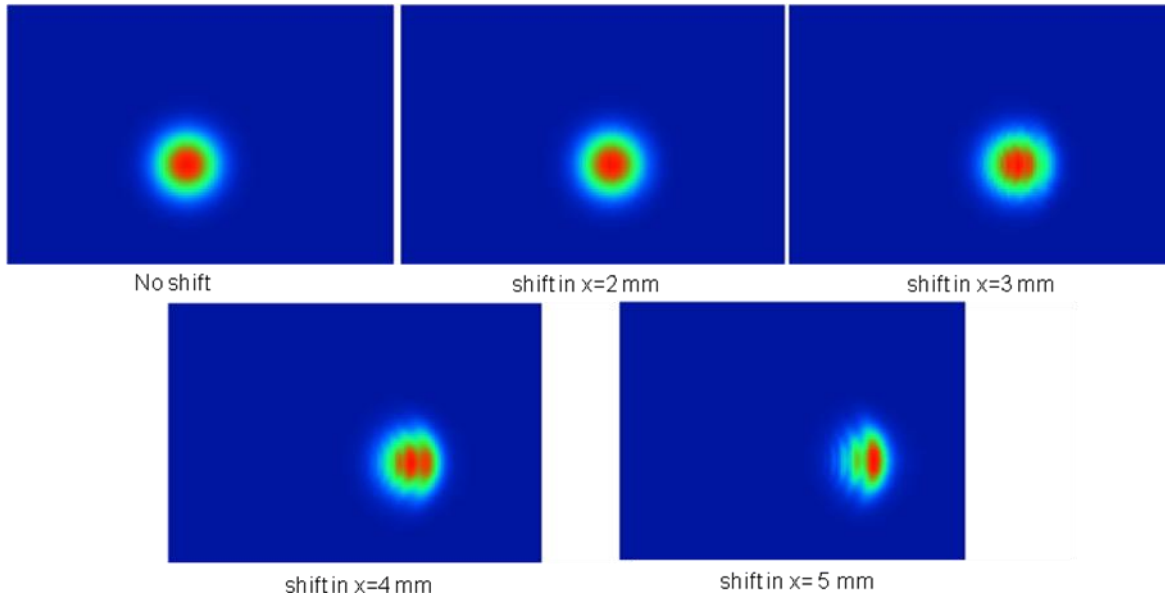


Figure 42: B2 beam shape versus shift of the beam on SIB_M5 mirror .

It seems according to that result that the problem comes mainly from a beam shift. The beam shift produces that strange beam shape when the input beam is shifted by more than 3 mm.

A shift of about 4-5mm can produce the very bad beam that we observed experimentally (see figure 40).

The first thing to try is to move the beam using the BMS with about 1-2mm shift the situation should really be improved.

On the figure 42, one can see the beam shape when we have a shift of 3 mm. The situation seems to be a bit better.

Zemax software helped us a lot to understand what we had to do to correct astigmatism on the ITF for example. In particular we have studied extensively the compensation of astigmatism on the interferometer after M6 tilt and we came to the conclusion that we had to rotate it.

We could also explain in an easy way strange beam shape of the ITF reflection after the relocking of the IMC just after the SIB installation [2].

7.3. Use of Zemax software for matching adjustment on Virgo+: Example 2.

After the installation of the Virgo+ mirrors in spring 2010, due to some problems of asymmetry of the cavities and different cavity waist size respect to Virgo, we had to retune the beam size at the ITF input port in order to have a matching on north and west cavities as close as possible. For VIRGO 3km-long Fabry-Perot cavities the optimal waist size was about 21 mm located on the input mirrors. For Virgo+, the optimal beam size at the cavity input mirrors has been estimated to be about 18.4mm [3][4].

In order to understand how the telescopes of the SIB have to be tuned we used Zemax software. On figure 43, one can see the beam waist size at the output of the SIB (color scale) when the beam waist is maintained on the arm cavities input mirrors changing the distance between the 2 lenses of T1 telescope (surface 3) and changing the distance between the 2 mirrors of the parabolic telescope

(surface 15). Figure 43 tells us that in order to adjust the beam in the right way, we have to decrease the distance between the 2 mirrors of the parabolic telescope and at the same time increase the distance between the 2 lenses of T1 telescope.

After having measured the mismatching before any action (mismatching was around 8% on the north cavity and 5% on the west cavity), we have adjusted the 2 telescopes in the direction foreseen with Zemax simulation. We measured again the mismatching on North and west cavities and we found a mismatching of 3% on the north cavity and 2% on the west cavity (see logentry [#26887](#) for more details).

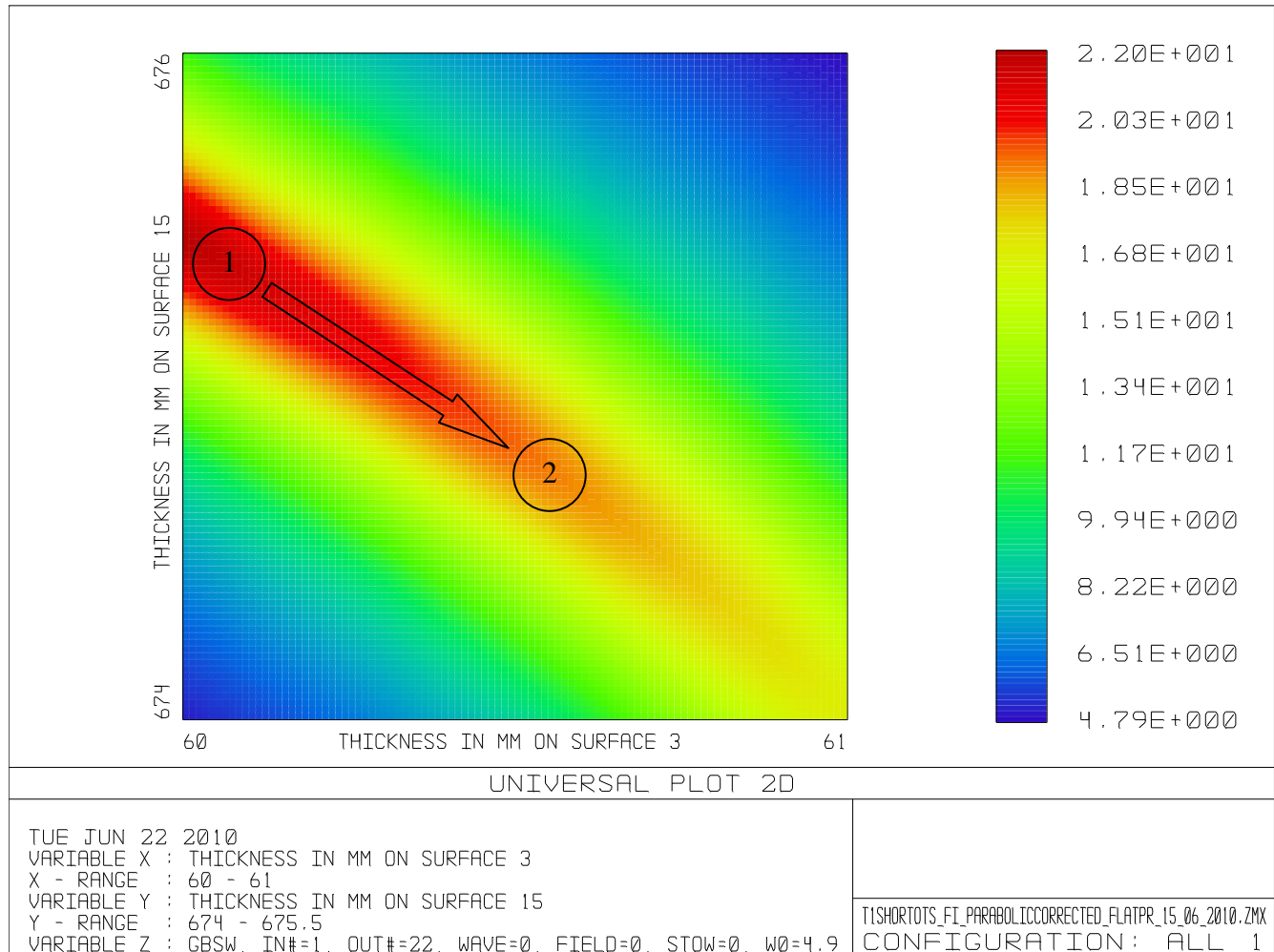


Figure 43: Waist size of the beam located on Fabry-Perot cavities input mirrors versus the distance between T1 telescope lenses and T2 telescope mirrors.

8. Appendix A: Parabolic mirrors optical characterization

8.1. M5 mirror

On figure 44, the characterization of M5 mirror after its production by Optical surfaces Ltd is given. As written in the datasheet [5], the micro-roughness is quite bad (0.9 nm r.m.s) and responsible for high scattering of the order of 90 ppm measured by LMA.

Mirror characteristic	Value
Diameter	50.74 mm
Thickness	14.95 mm
Focal length	74.48 mm
Flatness	10 nm r.m.s
Micro-roughness	0.9 nm r.m.s.
Scattering	89 ppm
Coating absorption	0.6 ppm
Mirror transmission	87 ppm @ 5° A.O.I

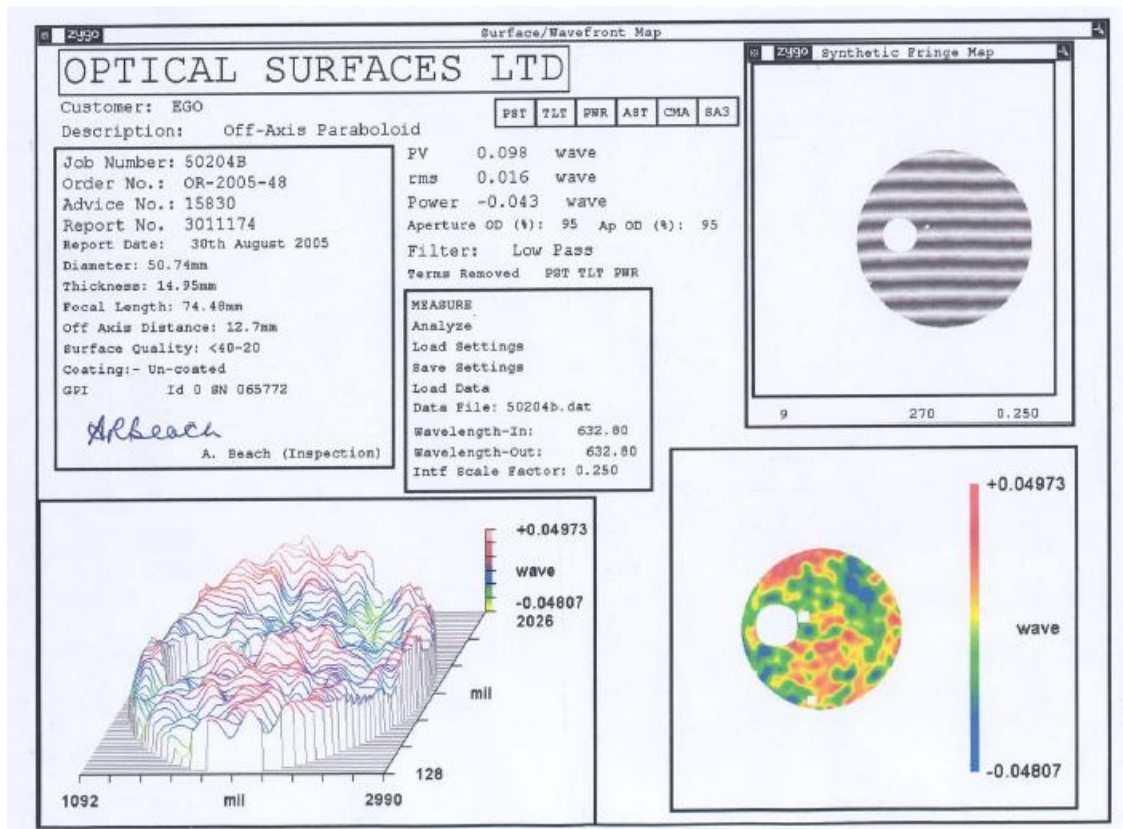


Figure 44: Un-coated M5 mirror characterization by Optical surfaces ltd.

8.2. M6 mirror

On figure 45, the characterization of M6 mirror after its production by Optical surfaces Ltd is given. As written in the datasheet [6], the micro-roughness is quite bad (1.5 nm r.m.s) and responsible for high scattering of the order of 320 ppm measured by LMA.

Mirror characteristic	Value
Diameter	114.5 mm
Thickness	30.75 mm
Focal length	604 mm
Flatness	8.2 nm r.m.s
Micro-roughness	1.5 nm r.m.s.
Scattering	320 ppm
Coating absorption	0.6 ppm
Mirror transmission	8 ppm @ 3° A.O.I

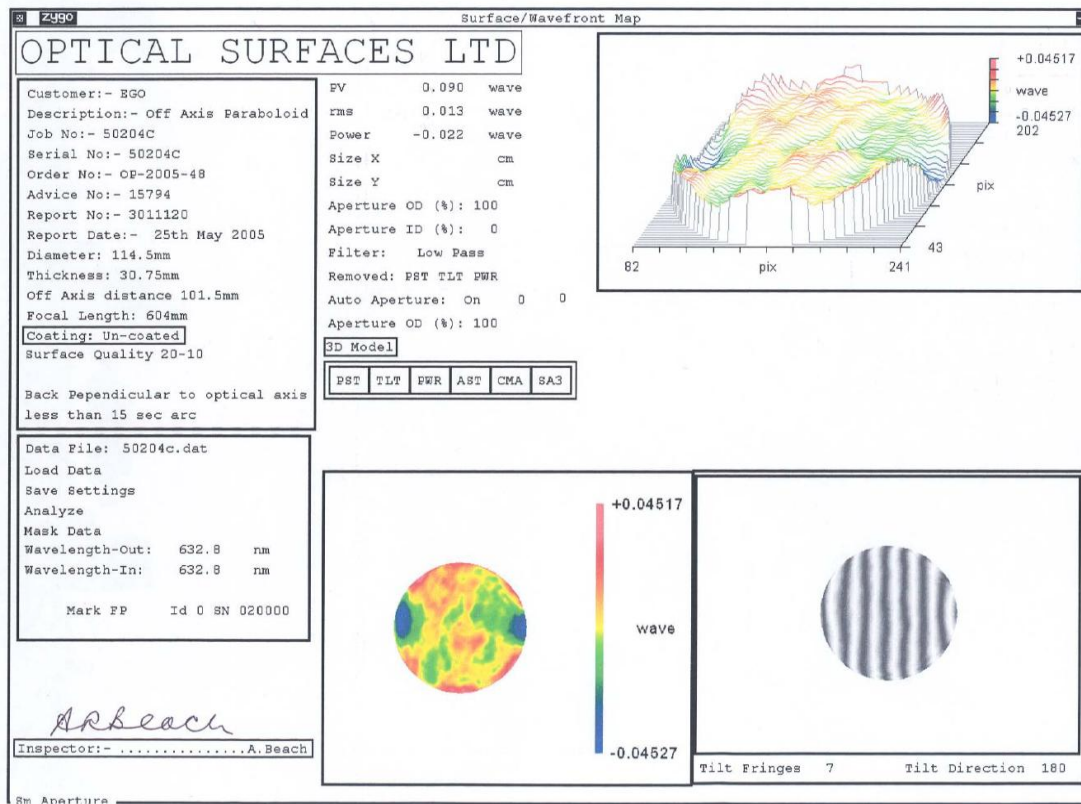


Figure 45: Un-coated M6 mirror characterization by Optical surfaces ltd.

9. Appendix B : Mirrors mechanical mounts.

A view of the parabolic telescope as designed with mirror mechanical mounts is given on figure 46.

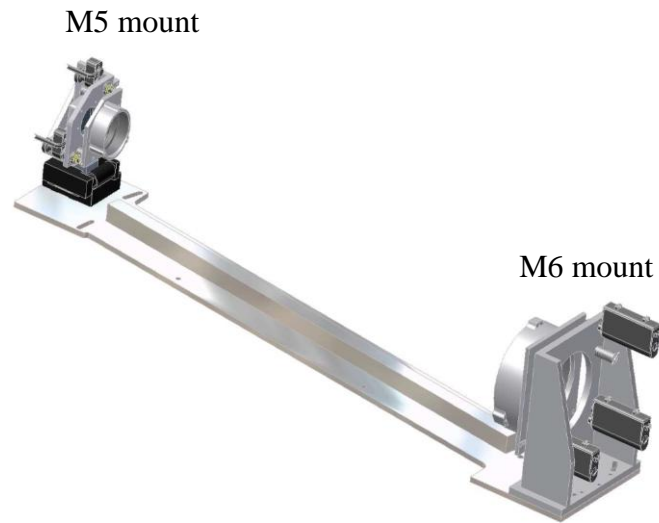


Figure 46: Parabolic telescope mechanical layout.

10. Appendix C : actuators

All the actuators installed are vacuum compatible. The specified vacuum level is 10^{-6} mbar (short towers vacuum level). The most critical components to be controlled have been identified with:

1. Lens distance of the T1 telescope (for controlling the collimation on the Faraday once the bench is in vacuum);
2. Lateral and longitudinal translations of the first mirror of the T2 parabolic telescope (M5, the 75 mm focal length one, to align the parabolic telescope);
3. Angles of the last mirror of the T2 parabolic telescope (M6 mirror (600 mm focal length mirror), to steer the beam into the ITF).

For these mirrors it has decided to use closed-loop actuators, which allow a better repeatability and precision.

9.1. Plane mirror actuators


For these mirrors the use of New Focus 8831 picomotors allows a dynamic range of 0.2 rad and a minimum step (resolution) of about 1 nrad. The dynamic range is much more than expected (a few mrad), and the minimum step is also much below the needs. These motors have been tested since long in Virgo: if they are used with the factory treatment they have resulted reliable. Other actuators (e.g. stepping motors) have been taken into account, but all the other possibilities were too big to fit on the bench.

9.2. Parabolic mirror angular actuators

The same actuators New Focus 8831 picomotors are going to be used on the first mirror of the parabolic telescope T2 (M5): once the bench and the telescope is aligned, it is not expected to need to realign this mirror. To steer the beam it is planned to use the second mirror of T2 (M6). Since the angular alignment of this mirror is not critical, M5 will be mounted on two 8831 picomotors.

The second mirror of T2 (M6) should be used to steer the beam into the ITF once the telescope and the bench are aligned. The allowed dynamics before mismatching the T2 telescope is globally 1 mrad. We have decided to mount M6 on three New Focus closed-loop 8810 picomotors: this will allow a better repeatability and reproducibility of the movements of this mirror: the positioning accuracy and repeatability of these actuators are respectively 63nm and ± 1 μ m over the full travelling range. The reproducibility, in particular, is very important to allow alignment procedures, without the risk of losing the good position. This is a critical problem of the 8831 picomotors, which unpredictable positioning hysteresis is well known. The impossibility to do this has been a major drawback in the old IB. The total dynamics of the 8810 picomotors is analogous to the 8831 ones (i.e. 0.2 rad), which is much more than the need (a few milliradians maximum).

Since M6 will be used only to steer the beam (it could also be translated by moving all the three picomotors at the same time), the possible needed translations of the axis of the T2 telescope will be performed acting on M5. This mirror will be mounted on three PI M-111 translators, so that all the x-

	<p>Note on Virgo Parabolic telescope</p>	<p>Date 09/2010 VIR-0504A-10 Page 58 of 59</p>
--	--	--

y-z movements are allowed. This is necessary in order to align the telescope if it turns out that the alignment in air was not correct and in case of unexpected misalignments after the suspension of the bench in vacuum and because possible unexpected thermal effects in the Faraday Isolator. In particular, the focalization of the T2 telescope will have to be checked to maximize the matching between the beam and the telescope. This will be done by changing the longitudinal distance of M5 and M6 (the distance along the axis of the bench): in this case a movement of no more than some tens of μm is expected. The global possible movements will not exceed some mm, and a resolution of $0.1 \mu\text{m}$ is necessary.

The PI M-111 actuators are closed-loop, with a dynamics of about 10 mm. The nominal resolution is some tens of nm, which is better than the required one.

9.3. Lens translator


The distance between the L1 and L2 lenses of the T1 telescope has to be controlled, in order to correct possible mismatching produced by the placing in vacuum of the bench and by unexpected thermal effects in the Faraday Isolator or in the Input Mode Cleaner cavity. A dynamics of not more than 1 mm is required. A resolution of one μm is sufficient. No transverse actuation on the T1 lenses is designed (i.e. no angular and lateral remote correction). One of the two lenses (L2, for space constraints) will be mounted on a PI M-111 translator. Also in this case, the dynamics and resolution of this actuator meet the specifications.

9.4. PZT for the RFC steering mirrors

The need of mounting the last two steering mirror of the RFC comes from the new Injection System alignment scheme. In this scheme it will be necessary to align the RFC and the IMC separately. Since the RFC is mounted below the IB, and no plan has been made to move it from this position, the beam that goes to this cavity has to be steered with separate actuators.

Several possibilities have been considered (e.g. the use of galvanometers), but it has turned out that the simplest solution was to use PZT. The choice has fallen on the PI S-330.2SL modified PZT actuators. The dynamic range of these actuators is some mrad, with a resolution better than one μrad . The position is controlled by an encoder, which gives a closed-loop reading of the mirror position. They can be controlled with feedback signals for RFC automatic alignment implementation.

The noise level required on the alignment of the beam on the RFC is at the level of 10^{-7} rad. According to company information and our experience with PI PAT actuators, we don't expect a thermal noise of the PZT larger than this figure. Moreover using low noise piezo drivers we should not create extra seismic noise that could spoil Virgo interferometer sensitivity.

	Note on Virgo Parabolic telescope	Date 09/2010 VIR-0504A-10 Page 59 of 59
--	-----------------------------------	---

11. References

- [1] J.D. Mansell et al, Appl.Opt., 40, 366-374, (2001).
- [2] Eric Genin, Paolo La Penna, Study of upper part telescopes: Astigmatism investigations, Virgo week April 2006, Commissioning meeting.
- [3] Massimo Galimberti, Raffaele Flaminio, Laurent Pinard, “Virgo+ arm cavities: Siesta simulations”, Commissioning weekly meeting, VIR-0381A-10, June 18, 2010.
- [4] A. Chiummo, R. Day, J. Marque, B. Swinkels, “Estimation of Radii of Curvature from mirror maps”, Commissioning weekly meeting, VIR-0401A-10, June 18, 2010.
- [5] LMA, M5 mirror characterization after coating,
http://wwwcascina.virgo.infn.it/optics/doc_optics/SIB_M5_LMA2005.pdf
- [6] LMA, M6 mirror characterization after coating,
http://wwwcascina.virgo.infn.it/optics/doc_optics/SIB_M6_LMA2005.pdf